



New middle Eocene omomyines (Primates, Haplorhini) from San Diego County, California

Amy L. Atwater^{a, b, *}, E. Christopher Kirk^{a, c}

^a Department of Anthropology, University of Texas at Austin, 2201 Speedway Stop C3200, Austin TX 78712, USA

^b Museum of the Rockies, Montana State University, 600 W Kagy Blvd., Bozeman, MT 59717, USA

^c Jackson School Museum of Earth History, University of Texas at Austin, J. J. Pickle Research Campus, 10100 Burnet Road, PRC 6-VPL, R7600, Austin, TX 78758, USA

ARTICLE INFO

Article history:

Received 21 September 2017

Accepted 16 April 2018

Available online 24 August 2018

Keywords:

Omomyoidea

Omomyidae

Omomyinae

Tarsiiformes

Uintan land mammal age

Friars Formation

Bayesian phylogenetics

ABSTRACT

The Friars Formation of San Diego County, California, has yielded a middle Eocene mammalian fauna from the early part of the Uintan North American Land Mammal Age. Prior research on the primate fauna from the Friars Formation provides evidence of one notharctine and multiple omomyine species, but many specimens collected since the early 1980s remain unstudied. Here we describe three new omomyine genera from the Friars Formation. These new taxa range in estimated body mass from about 119 g to 757 g, and substantially expand the diversity of middle Eocene omomyoids known from Southern California. Resolution of the phylogenetic relationships of the new Friars Formation omomyines is complicated by the fact that different character-taxon matrices and tree building methods produce different results. Nevertheless, all preliminary phylogenetic analyses are congruent in recovering a close relationship between the three new genera and the omomyines *Macrotarsius*, *Omomys*, *Ourayia*, and *Utahia*. Prior research has documented a shift in omomyoid diversity in North America from the anantomorphine-rich Bridgerian to the omomyine-rich Uintan. Our description of three new Uintan omomyine taxa from the Friars Formation further emphasizes these opposite trends in anantomorphine and omomyine species richness during the middle Eocene. All three of the new taxa are currently known from only the Friars Formation in San Diego County, California. Four of the previously known omomyoid genera from Southern California (*Dyseolemur*, *Chumashius*, *Yaquiuis*, and *Stockia*) are also endemic to the region, further highlighting the provincial character of primate faunas in Utah, Southern California, and West Texas during the Uintan.

© 2018 Elsevier Ltd. All rights reserved.

1. Introduction

The Friars Formation of Southern California has produced a middle Eocene fauna from the early Uintan North American Land Mammal Age (NALMA¹) that includes both adapiform and omomyoid primates. The first primate fossils from the Friars Formation were described by Stock (1933), who named *Yumanius woodringi* on the basis of a holotype partial maxilla with M1-2 and two

fragmentary paratype mandibles. Gazin (1958) subsequently synonymized *Yumanius* with *Washakius*, and noted that Stock's *Yumanius* paratypes could not represent the same taxon as the *W. woodringi* holotype. Gazin accordingly allocated the *Yumanius* paratype mandibles to a new taxon: *Stockia powayensis* (Gazin, 1958). Lillegraven (1980) provided the next major review of fossil primates from Southern California following renewed collecting in the late 1960s by field parties from the University of California Berkeley and San Diego State University. Lillegraven (1980) identified only three crown primate taxa from the Friars Formation, all of which are omomyoids: *S. powayensis*², *W. woodringi*, and “? *Macrotarsius* sp. near *M. jepseni*”. According to Lillegraven (1980),

* Corresponding author.

E-mail addresses: amy.atwater@montana.edu (A.L. Atwater), eckirk@austin.utexas.edu (E.C. Kirk).

¹ Abbreviations used in the text are: NALMA, North American Land Mammal Age; SDNHM, San Diego Natural History Museum; i = mandibular incisor; I = premaxillary incisor; c = mandibular canine; C = maxillary canine; p = mandibular premolar; P = maxillary premolar; m = mandibular molar; M = maxillary molar; L = maximum mesiodistal tooth length; W = maximum buccolingual tooth width (all measurements are in millimeters).

² Lillegraven (1980) considered *Stockia* to be synonymous with *Omomys*. Here we follow most subsequent authors in recognizing *Stockia* as a valid genus distinct from *Omomys* (e.g., Honey, 1990; Walsh, 1996).

all three of these taxa are also present in the overlying late Uintan faunal assemblage from the Mission Valley Formation. However, in conjunction with a revision of the stratigraphy of San Diego County (Walsh et al., 1996), Walsh (1996) concluded that *Stockia* is represented in only the Friars Formation and that *W. woodringi* occurs in only the Friars Formation and the age-equivalent Member B of the Santiago Formation.

The first adapiform fossils from the Friars Formation were described by Gunnell (1995), who named the new notharctine taxon *Hesperolemur actius* on the basis of a cranium and two isolated lower molars. Rose et al. (1999) subsequently questioned the validity of *Hesperolemur* and suggested that the Friars Formation notharctine sample could be accommodated within the genus *Cantius*. The *Hesperolemur* hypodigm is part of a larger sample of primate fossils collected in the 1980s and 1990s by San Diego Natural History Museum (SDNHM) field crews directed by Stephen L. Walsh (Walsh, 1996). Although Walsh never formally described the omomyoid fossils in this sample, he clearly recognized that it included taxa not previously identified from the Friars Formation. In his 1996 review of Eocene mammals from San Diego County, Walsh provided the following list of primate taxa from the Friars Formation: *Hesperolemur*³, *Stockia*, *Washakius*, “*Ourayia* sp(p). unidentified”, “*Hemiacodon* sp. near *Hemiacodon gracilis*”, and “*Omomyys* cf. *Omomyys carteri*” (Walsh, 1996, p. 84). Furthermore, many of the SDNHM specimens described in the present paper were originally cataloged by Walsh in the early 1990s and labeled “*Ourayia* sp. nov.” and “*Omomyys* sp. nov.”, providing further evidence that Walsh provisionally allocated these new specimens from the Friars Formation to known genera.

Having examined the SDNHM primate sample from the Friars Formation, we agree with Lillegraven (1980) and Walsh (1996) that multiple omomyoid genera are represented in addition to *Stockia* and *Washakius*. After detailed comparisons with known species, however, we believe that much of this fossil material cannot be accommodated within existing omomyoid taxa. Accordingly, the goal of this paper is to describe three new genera representing the bulk of the undescribed SDNHM omomyoid sample from the Friars Formation. By documenting the existence of these new taxa, we do not seek to offer an exhaustive account of the omomyoid community of the Friars Formation, but instead to provide an incremental step in augmenting our knowledge of Uintan primate diversity in Southern California. We also aim to gain a better understanding of the evolutionary relationships of the new taxa, and explore the implications of this research for North American patterns of species richness during the middle Eocene.

2. Geology

The middle Eocene strata of San Diego County are composed of mammal-bearing fluvial deposits interfingering with fossiliferous marine deposits (Fig. 1; Walsh et al., 1996). In southwestern San Diego County, four successive lithostratigraphic units – the Friars Formation, Stadium Conglomerate, Mission Valley Formation, and Pomerado Conglomerate – have yielded mammalian faunas spanning the Uintan NALMA (Walsh et al., 1996; Robinson et al., 2004). Referred to as the “Poway” sandstones and conglomerates in earlier published literature (e.g., Stock, 1933; Gazin, 1958), the Friars Formation was named by Kennedy and Moore (1971) for the vertebrate-bearing sandstones, siltstones, and mudstones that occur above the marine sandstones and siltstones of the Scripps Formation, and below the fluvial Stadium Conglomerate (Walsh

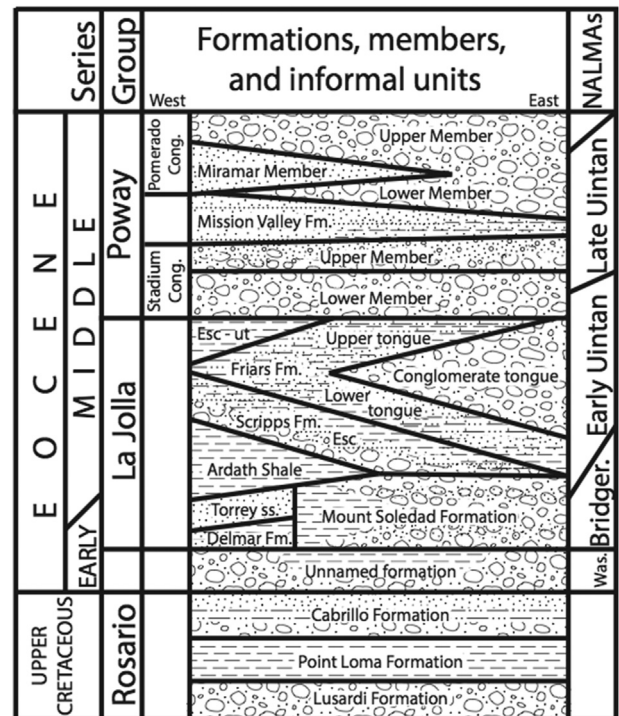


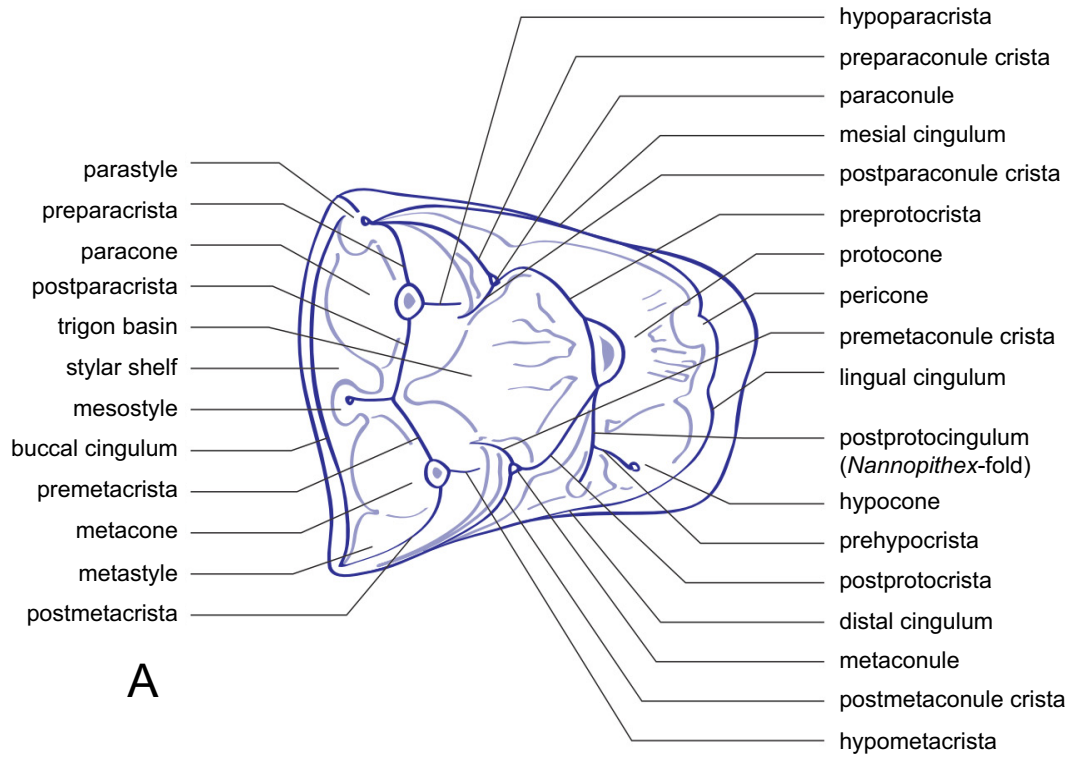
Figure 1. Stratigraphy of San Diego County. Modified from Walsh et al. (1996). Friars Formation lies stratigraphically above the Mount Soledad Formation and below the Stadium Conglomerate. Abbreviations: ut. = upper tongue; Esc.: Eocene Scripps Formation; ss. = sandstone; Fm. = Formation; Was. = Wasatchian; Bridger. = Bridgerian.

et al., 1996). The Friars Formation consists of three named sub-units (lower tongue, conglomerate tongue, and upper tongue) that are fluvial, deltaic, and lagoonal in origin, and which exhibit no readily observable differences in faunal content (Walsh, 1996; Walsh et al., 1996). All three units of the Friars Formation have produced an early Uintan mammal fauna (Ui1b), marked by the presence of *Leptoreodon*, *Protoreodon*, and other selenodont artiodactyls, as well as a range of Uintan index taxa such as *Amyrnodon* and *Achaenodon* (Walsh, 1996; Robinson et al., 2004; Gunnell et al., 2009). Although the absolute age of the Friars Formation is unknown at present, magnetostratigraphic analyses place the lower Friars Formation in Chron C21n and the upper Friars Formation in Chron C20r (Flynn, 1986; Bottjer et al., 1991). If correct, these correlations suggest an absolute date for the Friars Formation of approximately 46–44 Ma. These dates are congruent with the early Uintan fauna from the Friars Formation, since the Uintan encompasses a time interval between about 46.2 Ma and 40 Ma (Robinson et al., 2004). An absolute date of about 46–44 Ma for the Friars Formation is also consistent with an Ar/Ar date of 42.83 ± 0.24 Ma in the overlying Mission Valley Formation, which has produced a late Uintan faunal assemblage (Walsh, 1996; Walsh et al., 1996).

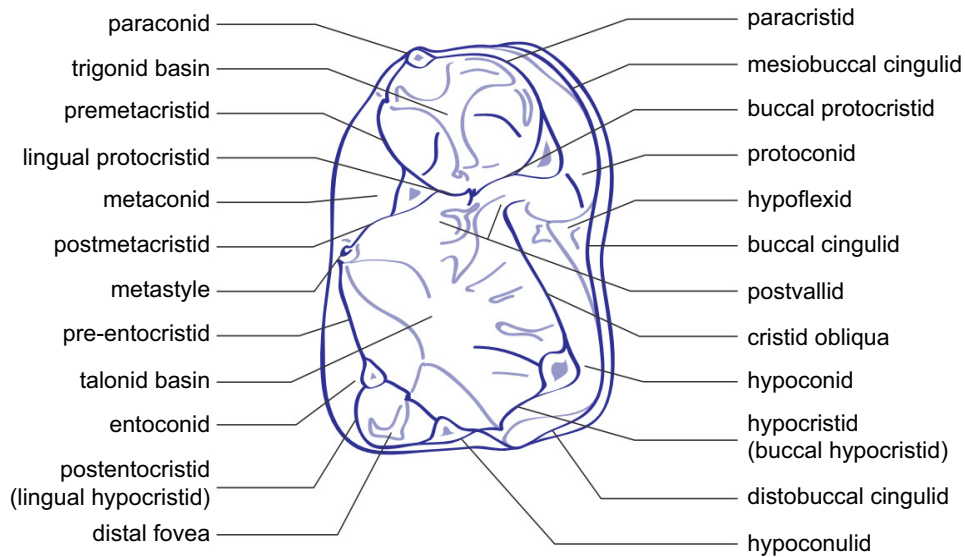
3. Materials and methods

All of the new omomyoid fossils described here are housed in the collections of the Department of Paleontology at the SDNHM. With the exception of *Diablomomys dalquesti*, comparisons with other fossil taxa were based primarily on the study of epoxy resin casts, supplemented by published photographs and drawings (Gazin, 1958; Szalay, 1976; Beard, 1987; Mason, 1990; Williams and Kirk, 2008). Nomenclature used for dental morphology largely follows that of Ni et al. (2016) with some modifications and is illustrated in Figure 2.

³ Identified as “Adapidae, new gen. and sp. [G. Gunnell, in press]” (Walsh, 1996, p. 84).



A



B

Figure 2. Dental nomenclature. A, right upper molar. B, right lower molar. Modified from Ni et al. (2016).

Most dental dimensions were measured to the nearest 0.01 mm using Mitutoyo digital calipers. Additionally, all specimens were digitally photographed with a scale bar using a Leica M80 Microscope equipped with a Leica IC80 HD camera. When caliper measurements were not possible for teeth in situ in either the mandible or maxilla, measurements were taken from digital photographs using the line segment and measure tools in ImageJ (Schneider et al., 2012). Body mass was estimated using the “all primate”

and “prosimian” least-squares regression equations presented in Conroy (1987). These equations are:

$$\text{All Primate: } \ln(B) = 1.784 \ln(A) + 2.54 \text{ (standard error } \pm 0.33)$$

$$\text{Prosimian: } \ln(B) = 1.614 \ln(A) + 2.67 \text{ (standard error } \pm 0.22)$$

In these equations, B is body mass in grams and A is the area of the m1 in millimeters. The m1 area is calculated as the product of

tooth crown length and width (Conroy, 1987; Kirk and Simons, 2001).

3.1. CT scans

Twenty-four specimens were selected for micro-computed tomography (CT) scanning at the High-Resolution X-ray Computed Tomography Facility at The University of Texas at Austin. Two mandibular specimens of the largest new taxon described here (SDNHM 55253 and SDNHM 55252) were scanned using a North Star Imaging (NSI) scanner at 15.2 micron voxel resolution. Eight specimens of the smallest new taxon (SDNHM 105007, SDNHM 96637, SDNHM 39750, SDNHM 55168, SDNHM 141153, SDNHM 31649, SDNHM 39756, SDNHM 39758), six specimens of the intermediate-sized new taxon (SDNHM 38126, SDNHM 55250, SDNHM 56991, SDNHM 87871, SDNHM 46439, SDNHM 43094), and eight specimens of the largest new taxon (SDNHM 60683, SDNHM 60681, SDNHM 58005, SDNHM 55819, SDNHM 60684, SDNHM 60671, SDNHM 56700, SDNHM 58008) were scanned with an Xradia microXCT scanner at 7.34 micron resolution. VGStudio 3.0 was used for image processing. All CT scan files and additional data on scanning parameters are available at www.morphosource.org.

3.2. Phylogenetic analyses

Our phylogenetic analyses were based on two different character-taxon matrices: Ni et al. (2016) and Tornow (2008). The Ni et al. (2016) matrix includes 1890 characters scored for 196 taxa. Here we pared the Ni et al. (2016) matrix to include only 510 dental characters. We also limited the taxa included to 27 North American omomyoid species, four European microchoerid species, *Teilhardina asiatica*, and *Teilhardina belgica* (Appendix A). We then added character scorings for the three new omomyoid genera described in this paper, as well as four additional North American genera that were not included in the Ni et al. (2016) matrix: *Yaqui* *travisi*, *S. powayensis*, *D. dalquesti*, and *Utahia kayi*. The Tornow (2008) matrix includes 100 characters, (76 dental and 24 cranial and postcranial characters) scored for 25 North American omomyoid taxa. We added character scorings for the three new omomyoid genera described in this paper. Tornow (2008) uses generalized gap coding to convert quantitative data into discrete character states, and the new taxa described here were scored using these previously identified states. Editing of both character-taxon matrices and generation of the final NEXUS files for our phylogenetic analyses was accomplished in Mesquite v3.2 (Maddison and Maddison, 2017).

Parsimony analysis of the two resulting character-taxon matrices (hereafter referred to as the “Ni” and “Tornow” matrices) was undertaken using PAUP* (Swofford, 2003). For each matrix, we ran a heuristic search under the parsimony criterion with 100,000 random addition sequence replicates, with random starting trees, and swapping using TBR. We then applied the bootstrap resampling method to the resulting majority-rule consensus tree. The bootstrap analysis consisted of generating 1000 pseudoreplicate trees. For each pseudoreplicate tree, PAUP* performed a heuristic search and retained all groups in the majority-rule consensus tree, including those with less than 50% support. All characters were assigned equal weight. Characters were treated as ordered or unordered (Appendix A). Outgroups selected for parsimony analyses included *T. asiatica* for the Ni matrix, and *Teilhardina americana* for the Tornow matrix.

Additionally, Bayesian phylogenetic analyses of the Ni and Tornow matrices were undertaken using MrBayes v3.2.6 (Ronquist et al., 2012). The most widely used model for estimating phylogenetic trees from discrete phenotypic data is the Mk model proposed by Lewis (Lewis, 2001; Wright and Hillis, 2014). The Mk model

assumes a Markov process for character change, which allows for multiple character-state changes along a single branch (Wright and Hillis, 2014). For our analyses, MrBayes used the Mk model with the Dirichlet distribution parameter fixed to 1.0, which allows for a uniform prior on the proportions of the state frequencies (Ronquist et al., 2005). A gamma-distributed rate model, a random start tree, and a consensus tree output were selected. The Ni matrix ran for 3,500,000 mcmc generations, with a sample frequency of 500 in order to maximize sampling from the posterior probability. The Ni matrix analysis used two chains with a temperature of 0.025. *T. asiatica* was selected as the outgroup for the Bayesian analysis of the Ni matrix. The Tornow data matrix ran for 2,000,000 mcmc generations, with a sample frequency of 500. The number of chains was set to two, and the chain temperature equals 0.017. *T. americana* was chosen as the outgroup for the Bayesian analysis of the Tornow matrix.

4. Results

4.1. Systematic paleontology

Order Primates Linnaeus, 1758
 Semiorder Haplorhini Pocock, 1918
 Infraorder Tarsiiformes? Gregory, 1915
 Superfamily Omomyoidea Trouessart, 1879
 Family Omomyidae Trouessart, 1879
 Subfamily Omomyinae Trouessart, 1879
Ekwiemakius, gen. nov.
 Type species: *E. walshi*, sp. nov.

Generic diagnosis Omomyine primate that differs from other North American omomyoids except *Diablomomys*, *Macrotarsius*, *Omomys*, and *Rooneyia* in lacking a postprotocingulum on the upper first molar. Differs from all other North American omomyoids except *Rooneyia* and *Washakius* in the presence of a deep sulcus between the protocone and hypocone of the M1-2. Length and width measurements of the upper and lower dentition are absolutely smaller than *Chumashius*, *Diablomomys*, *Macrotarsius*, *Mytonius*, *O. carteri*, *Ourayia*, *Stockia*, *Utahia*, and *Yaqui* *travisi*, similar in size to *W. woodringi* and specimens attributed to *Omomys lloydi*, and larger than *Dyseolemur*. Differs from *Omomys* in having an M1 that lacks a pericone, having a discontinuous lingual cingulum, and in having larger conules. Further differs from *Omomys* in having a more waisted distal margin of the M1-2, and in lacking a lingual cingulid on the p3-4. Differs from *Stockia* and *Utahia* in having a lingually positioned m2 paraconid that is lower in height relative to the metaconid, in having lower molar trigonids that are less mesiodistally constricted, and in having m2-3 trigonids that are more open lingually. Further differs from *Stockia* in having a well-developed p4 metaconid. Differs from *Yaqui* *travisi* in having a p3 that lacks a buccal or mesiobuccal cingulid, and in having a relatively mesiodistally longer p4 with a cusped paraconid. Further differs from *Yaqui* *travisi* in having an m1 paraconid that is buccolingually positioned between the protoconid and metaconid. Differs from *Diablomomys* in the presence of the postmetaconule crista on the M1-2, in having a larger M1 hypocone, and in having an M2 with a waisted distal margin. Also differs from *Diablomomys* in having a p4 with a mesiodistal length similar to that of the m1 and a p4 metaconid height that is much lower relative to the height of the protoconid. Differs from *Macrotarsius* and *Ourayia* in lacking crenulated enamel and in having upper molars that lack a mesostyle and exhibit weakly developed distal and mesial cingula. Differs from *Mytonius* in having a mesiodistally longer p4, a greater height difference between lower molar trigonids and talonids, less bunodont lower molar cusps, and a more lingually positioned M2

paraconid. Differs from *Washakius* in having upper molars with smaller conules and a continuous postprotocrista between the protocone and metaconule. Differs from *Rooneyia* in having smaller upper molar conules and hypocones. Differs from *Chumashius* in having a p4 with a larger paraconid and metaconid, an M2 with a prominent hypocone, and an M3 that is buccolingually wider.

Etymology Derived from the Kumeyaay place name ‘Ekwiymak’ (“behind the clouds”) for the Cuyamaca region of eastern San Diego County that contains the headwaters of both the San Diego and Sweetwater rivers. The Kumeyaay people have inhabited San Diego County for over 475 years, and were the first Native Americans to greet explorer Juan Cabrillo when he arrived in San Diego Bay in 1542.

Ekwiymakius walshi, sp. nov. (Fig. 3, Table 2).

Holotype SDNHM 31649, isolated M1.

Paratypes SDNHM 96637, isolated p4; SDNHM 39750, isolated m1; SDNHM 55168, isolated m2; SDNHM 141153, isolated m3; SDNHM 96639, isolated M1; SDNHM 39756, isolated M2; SDNHM 39758, isolated M3.

Hypodigm SDNHM 55111, SDNHM 105007, SDNHM 46365, isolated p4s; SDNHM 96638, SDNHM 87822, isolated m1s; SDNHM 105356, isolated m2; SDNHM 39751, SDNHM 39752, SDNHM 55310, SDNHM 76983, SDNHM 39753, isolated m3s; SDNHM 105008, isolated P3; SDNHM 85697, isolated M1; SDNHM 39757, SDNHM 39352, SDNHM 39755, SDNHM 46138, isolated M2s; SDNHM 96642, SDNHM 31642, isolated M3s.

Horizon Lower, conglomerate, and upper tongues of the Friars Formation.

Specific diagnosis As for genus.

Etymology Named for Stephen L. Walsh, former SDNHM paleontologist, in recognition of his exceptional contributions to our understanding of the vertebrate paleontology and Eocene biostratigraphy of Southern California. Walsh collected and prepared many of the specimens described in this paper.

Description The p3 of *Ekwiymakius* has smooth enamel and lacks exodaenodontology. The p3 also lacks a metaconid, buccal cingulid, and mesiobuccal cingulid. The p3 paraconid is cingulid-like and mesiolingually positioned. The p3 talonid is mesiodistally

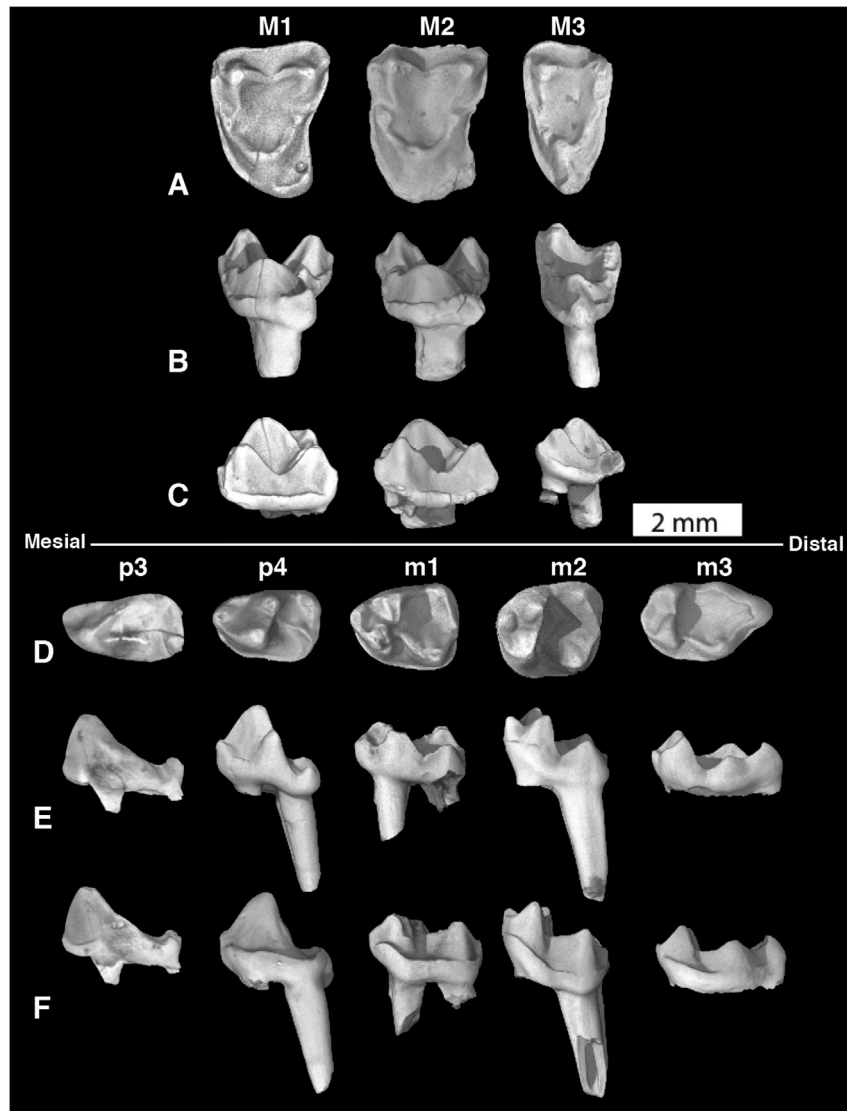


Figure 3. Upper and lower dentition of *Ekwiymakius walshi*. A–C: upper molars, A: occlusal view, B: lingual view, C: buccal view. D–F: lower dentition, D: occlusal view, E: lingual view, F: buccal view. M1: SDNHM 31649; M2: SDNHM 39756; M3: SDNHM 39758; p3: 105007; p4: SDNHM 96637; m1: SDNHM 39750; m2: SDNHM 55168; m3: SDNHM 141153. Note that some images have been digitally mirror-imaged to facilitate comparisons.

Table 1

Estimated body mass of fossil taxa based on m1 area. All estimates calculated using least-squares regression formulas presented in [Conroy \(1987\)](#). Estimated body mass (bold) and 95% confidence range (parentheses) are expressed in grams. Area of the m1 is calculated as the product of maximum mesiodistal length by maximum buccolingual width of the crown area.

Taxon	m1 area (mm ²)	All primate regression (g)	Prosimian regression (g)
<i>Ekwiymakius</i>	3.7	131 (124–138)	119 (113–125)
<i>Gunneltarsius</i>	6.4	348 (330–366)	289 (275–303)
<i>Brontomomys</i>	11.6	1008 (958–1061)	757 (719–796)

Table 2

Measurements of *Ekwiymakius walshi* dentition in millimeters. Length = maximum mesiodistal crown length; Width = maximum buccolingual crown width.

<i>Ekwiymakius walshi</i>			
Specimen number	Position	Length	Width
SDNHM 105007	p3	2.18	1.36
SDNHM 96637	p4	2.03	1.4
SDNHM 55111	p4	2.11	1.3
SDNHM 46365	p4	1.84	1.11
SDNHM 39750	m1	2.2	1.63
SDNHM 96638	m1	2.15	1.57
SDNHM 87822	m1	2.08	1.63
SDNHM 55168	m2	1.92	1.66
SDNHM 105356	m2	2.09	1.76
SDNHM 141153	m3	2.37	1.36
SDNHM 39752	m3	2.42	1.45
SDNHM 39751	m3	2.21	1.43
SDNHM 55310	m3	2.18	1.46
SDNHM 76983	m3	2.32	1.44
SDNHM 39753	m3	2.32	1.4
SDNHM 96639	M1	2.133	2.895
SDNHM 31649	M1	2.15	2.8
SDNHM 85697	M1	2.03	2.85
SDNHM 39756	M2	2.22	2.92
SDNHM 39757	M2	2.06	3.15
SDNHM 39342	M2	2	2.84
SDNHM 39755	M2	2.04	2.74
SDNHM 46138	M2	1.81	2.63
SDNHM 39758	M3	1.68	2.78
SDNHM 96642	M3	1.55	2.44
SDNHM 31642	M3	1.48	2.38

long while the trigonid is mesiodistally short. Width of the p3 is very narrow; buccolingual width is less than half of mesiodistal length. There is a sharp cristid present on the distobuccal wall of the p3 protoconid. The p4 has a metaconid that forms a small distinct cusp that is slightly distolingually positioned relative to the protoconid. The mesiodistal length of the p4 is shorter than that of the m1. The p4 paraconid is a distinct, small cusp that is positioned lingually. The p4 paracristid is sharp, but the mesial portion is not elevated and the buccal protocristid is distally oriented. The p4 has a lingual cingulid that is absent or weakly present, a weak mesio-buccal cingulid, and a strong buccal cingulid. The p4 hypoconid is heel-like and the entoconid is present as a small cusp. The p4 trigonid is proportionally shorter than the talonid, representing less than 40 percent of the total mesiodistal length. The lower molars of *Ekwiymakius* display well-developed buccal cingulids that are frequently discontinuous distally. The talonids of all lower molars are consistently wider than the trigonids. The m1 paraconid is a conical cusp that is positioned buccolingually between the protoconid and metaconid. The m1 metaconid is lower in height and distolingually positioned compared to the protoconid. The m1 trigonid is lingually open, and the paracristid is strong. The m1 entoconid is similar in size to the hypoconid. The m2 paraconid is a conical cusp that is lingually positioned mesial to the metaconid but is not basally fused with the metaconid. The m2 metaconid is distolingually positioned relative to the protoconid, and the m2 trigonid is lingually open. The m2 entoconid is similar in size to that

of the hypoconid. The m3 is mesiodistally longer than the m2. There is a single hypoconulid lobe on the m3 that is positioned near the midline. The upper molars of *Ekwiymakius* display a variably present discontinuous lingual cingulum and the M1-2 have a distinctly waisted distal margin. There is no postprotocingulum present on any of the upper molars. The M1 is smaller in size compared to the M2. The M1-2 have a well-developed conical hypocone that is distolingually positioned relative to the protocone. There is no pericone present on the M1, but a pericone is variably present on the M2. The M1-2 paraconule and metaconule are distinct but small in size. The M3 metaconule is much smaller in size compared to the paraconule. The M1-2 buccal cingula are strong, and the distal and mesial cingula are weakly developed. The M1-2 display a small but distinct parastyle and metastyle. The M1-2 also preserve a deep sulcus between the protocone and hypocone.

Discussion *Ekwiymakius* may be readily distinguished from the similar-sized omomyoid from the Friars Formation *W. woodringi* in its lack of the doubled metaconule, discontinuous postprotocrista, and distinct postprotocingulum characteristic of upper molars of *Washakius*. Among known omomyoid taxa, *Ekwiymakius* most closely resembles *Omomys*. Shared features of *Ekwiymakius* and *Omomys* include relatively smooth dental enamel, lack of a post-protocingulum on upper molars, presence of a waisted distal margin on the M1-2, variable size of the hypocone on the M1-2, and a variable presence of a pericone on the M2 ([Cuozzo, 2008](#)). *Omomys* and *Ekwiymakius* also share a p4 that has a well-defined but small metaconid, a mesiolingual cingulid, and a strong buccal and mesiobuccal cingulid. *Ekwiymakius* may be distinguished from *Omomys* in having an M1 with larger conules, a discontinuous lingual cingulum, and no pericone. *Ekwiymakius* also differs from *Omomys* in the presence of a deep sulcus between the protocone and hypocone on the M1-2, in having an M1-2 with a more distinctly waisted distal margin, and in having a p3-4 that lack a lingual cingulid.

Order Primates Linnaeus, 1758
 Semiorder Haplorhini Pocock, 1918
 Infraorder Tarsiiformes? Gregory, 1915
 Superfamily Omomyoidea Trouessart, 1879
 Family Omomyidae Trouessart, 1879
 Subfamily Omomyinae Trouessart, 1879
Gunneltarsius, gen. nov.
 Type species. *G. randalli*, sp. nov.

Generic diagnosis Omomyine primate that differs from all other North American omomyoids except *Diablomomys*, *Ekwiymakius*, *Macrotarsius*, *Omomys*, and *Rooneyia* in lacking an M1 post-protocingulum. Length and width measurements of the upper and lower dentition are absolutely smaller than *Diablomomys*, *Macrotarsius*, *Mytonius*, *Ourayia*, and *Yaquius*, similar in size to *Stockia* and *Omomys*, and larger than *Chumashius*, *Ekwiymakius*, *Utahia*, and *Washakius*. Differs from *Diablomomys*, *Macrotarsius*, *Omomys*, *Ourayia*, *Stockia*, and *Utahia* in having m2-3 trigonid lingual cusps that are lower in height relative to the protoconid. Differs from *Diablomomys*, *Ekwiymakius*, *Macrotarsius*, *Omomys*, *Stockia*, and

Utahia in having an m3 talonid that is similar in width relative to the trigonid. Differs from *Diablomomys*, *Ekwiymakius*, *Omomys*, and *Utahia* in lacking an m3 distobuccal cingulid. Differs from *Diablomomys*, *Ekwiymakius*, and *Omomys* in having moderate levels of upper and lower molar occlusal surface crenulation. Differs from *Ekwiymakius*, *Macrotarsius*, and *Omomys* in having an M1–2 with a narrow styler shelf. Differs from *Macrotarsius* and *Omomys* in having a P4 with a postprotocrista, and in having an M3 with a variably small or absent metacone. Differs from *Omomys* in having upper molars that are buccolingually broader in occlusal profile, in lacking overlapping premolars, and in having a small P3 protocone and P4 parastyle. Differs from *Mytonius* in having a mesiodistally longer p4 and a buccolingually narrower m2 with a more lingually positioned protoconid. Differs from *Macrotarsius* in having an M1 with a waisted distal margin and in having m1–2 metaconids that are relatively smaller than the protoconid. Differs from *Washakius* in having molars with weaker crenulation, and upper molars with smaller conules, smaller hypocones, a continuous lingual cingulum, and a continuous postprotocrista between the protocone and metaconule. Differs from *Ekwiymakius* in having an M1 with a continuous lingual cingulum, M2 lacking a waisted distal margin, a mesiodistally longer M3, and m1–3 with more lingually positioned paraconids. Differs from *Stockia* in having less crenulated lower molar occlusal surfaces, m1–3 trigonids that are mesiodistally longer, m2–3 paraconids that are positioned mesial to the metaconid, a smaller m3 hypoconulid, and an m3 entoconid that is weak and crestiform. Differs from *Chumashius* in having more lingually positioned lower molar paraconids, an M2 with a more distinct hypocone, pericone, and buccal cingulum, and a buccolingually wider M3 with a more similar-sized paracone and metacone.

Etymology Named for Dr. Gregg Gunnell in recognition of his extraordinary contributions to the study of Eocene mammals, through his extensive published research, mentorship of students, and collaborations with colleagues. In combination with *Tarsius*, acknowledging the probable stem haplorhine or stem tarsiiform phylogenetic affinities of the Omomyoidea.

Gunneltarsius randalli, sp. nov. (Fig. 4, Table 3).

Holotype SDNHM 38126, partial right mandible with p3–m1 and alveoli for i1, i2, c, and p2.

Paratypes SDNHM 55250, partial left maxilla, with complete P4, M1, and M3 crowns, the lingual half of the M2 crown, and alveoli for the P3; SDNHM 46439, isolated P3; SDNHM 43094, isolated M2; SDNHM 56991, isolated m2; SDNHM 87871, isolated m3.

Hypodigm SDNHM 31648, isolated P3; SDNHM 43097, SDNHM 38132, isolated P4s; SDNHM 38135, SDNHM 60667, SDNHM 43095, SDNHM 38134, SDNHM 60666, isolated M1s; SDNHM 37605, SDNHM 45826, SDNHM 31640, SDNHM 85942, SDNHM 56993, SDNHM 76981, isolated M2s; SDNHM 46560, SDNHM 55110, SDNHM 45827, SDNHM 87872, SDNHM 38136, SDNHM 37453, SDNHM 43096, SDNHM 38138, isolated M3s; SDNHM 58778, isolated p3; SDNHM 49270, partial mandible with m1–m2; SDNHM 60664, SDNHM 56990, SDNHM 85940, SDNHM 62283, SDNHM 51350, isolated m1s; SDNHM 55109, SDNHM 37600, SDNHM 60685, SDNHM 37599, SDNHM 60665, SDNHM 38129, isolated m2s; SDNHM 62224, SDNHM 56992, SDNHM 55445, SDNHM 37601, SDNHM 79804, SDNHM 85941, SDNHM 76982, SDNHM 40111, SDNHM 43814, isolated m3s.

Horizon Lower, conglomerate, and upper tongues of the Friars Formation.

Specific diagnosis As for genus.

Etymology Named for Kesler Randall, SDNHM Fossil Vertebrates Collections Manager, in recognition of his efforts to collect, prepare, and curate fossil mammals from San Diego County, and whose assistance with this project has been invaluable.

Description The holotype preserves single alveoli for the i1, i2, c, and p2. Neither incisor alveolus is intact, but both the i1 and i2 alveoli appear to have been ovoid and mesiodistally compressed. The i1 alveolus was also evidently much larger than the i2 alveolus. The c and p2 alveoli are more rounded than the incisor alveoli. The c alveolus is slightly larger than the p2 alveolus, but both of these alveoli are much larger than the i2 alveolus. The p3 of *Gunneltarsius* is moderately long, with the mesiodistal length greater than one half the length of the m1. The p3 protoconid is taller in height relative to that of the p4. The p3 buccal and mesiobuccal cingulids are weakly developed, and the p3 is lacking a lingual cingulid. The p3 paraconid is variable in form, being cingulid-like in some specimens, and forming a small distinct cusp in others. The p3 hypoconid is present as a short heel without a fully developed cusp, and the entoconid is variably absent or present. The p4 of *Gunneltarsius* has a mesiodistal length that is shorter than that of the m1. The p4 paraconid is absent, and the metaconid is present as a small distinct cusp. The p4 lingual cingulid is absent, while the mesiolingual cingulid is present but weak, and the buccal and mesiobuccal cingulids are strong. The p4 has a sharp ridge present on the distobuccal wall of the protoconid. The p4 hypoconid is present and heel-like but the entoconid is absent. The m1 paraconid is conical and is positioned mesial to the metaconid. The m1 metaconid is lower in height relative to the protoconid and is positioned distolingually relative to the protoconid. The m1 trigonid is lingually open. The m1–2 buccal and mesiobuccal cingulids are strongly developed. The m2 of *Gunneltarsius* has a conical paraconid that is positioned mesial to the metaconid. The m2 trigonid is lingually closed. The m3 is longer in mesiodistal length relative to the m1–2. The m3 talonid is similar in buccolingual width to the trigonid. The m3 hypoconulid is variable in position and in some specimens is subdivided into multiple small cusps. The m2–3 show moderate mesiodistal compression of the trigonid. The m1–3 talonids are lingually closed by a low cristid. The P3 paracone is taller in height relative to that of the P4. The P3 is lacking a metacone and has a small protocone that is more mesially positioned than the paracone. The P3 has a small parastyle, and is lacking a metastyle. The P3 has weak buccal and mesial cingula, is lacking a lingual cingulum, and has a strong distal cingulum. The P3 distal margin is waisted. The P4 protocone is more mesially positioned than the paracone, and its apex is displaced buccally from the lingual margin of the P4 crown. The P4 metacone and hypocone are absent. The P4 has a parastyle and lacks a metastyle. The P4 buccal, distal, and mesial cingula are strong, but the lingual cingulum is absent. The P4 distal margin is waisted, and the mesial margin is variably waisted. The M1 is smaller in size relative to the M2. The M1–2 hypocone is small and positioned distolingually relative to the protocone. The M1 has a small paraconule and metaconule, and has weak pre- and postconule cristae. The M1 has a slightly waisted distal margin. The M2 pericone and postprotocingulum are variably present, and the M2 distal margin is variably waisted. The M3 is small in size relative to the M1–2 and lacks a hypocone. The M1–3 have strong lingual cingula, and M1–2 have strong buccal cingula. The M1–2 have a small parastyle and metastyle, as well as a narrow styler shelf. The M1–2 also have strong mesial and distal cingula. The upper and lower molar occlusal surfaces are slightly crenulated.

Discussion In addition to the aforementioned differences in occlusal morphology, *Gunneltarsius* is easily discriminated from Friars Formation *Washakius* and *Ekwiymakius* by its larger size.

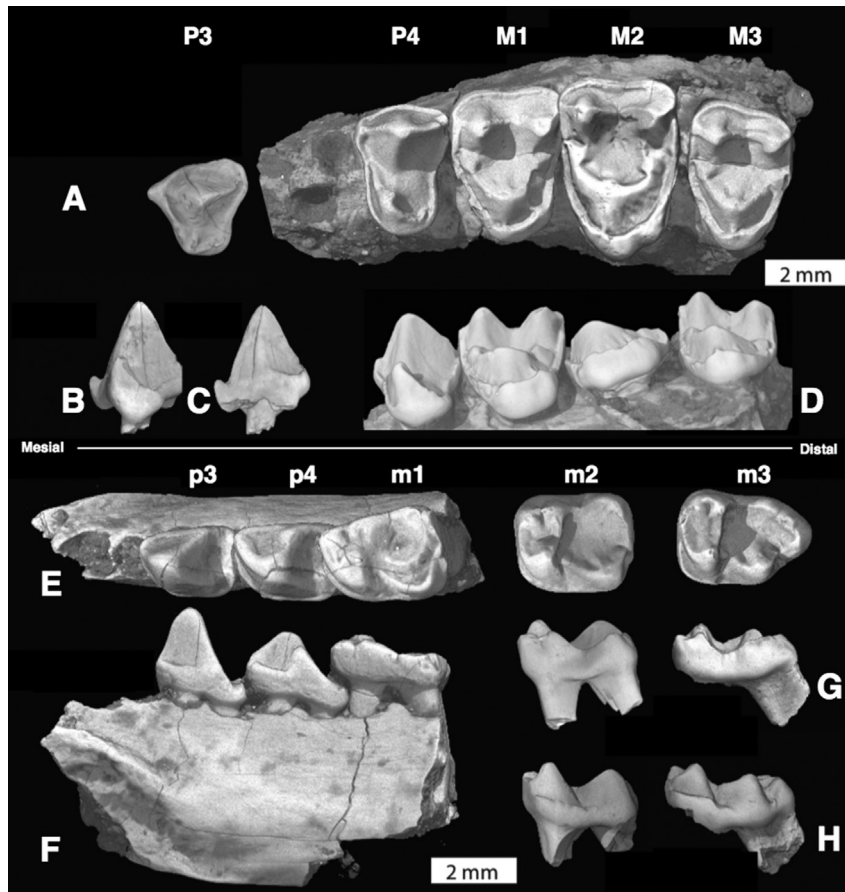


Figure 4. Upper and lower dentition of *Gunneltarsius randalli*. A–D: upper dentition, A: P3–M3 occlusal view, B: P3 lingual view, C: P3 buccal view, D: P4–M3 lingual view. E–H: lower dentition, E: p3–m3 occlusal view, F: p3–m1 lingual view, G: m2–m3 lingual view, H: m2–m3 buccal view. P3: SDNHM 46439; P4, M1, and M3: SDNHM 55250; M2: SDNHM 43094; p3–m1: SDNHM 38126; m2: SDNHM 56991; m3: SDNHM 87871. Note that some images have been digitally mirror-imaged to facilitate comparisons.

Occlusal morphology also readily distinguishes *Gunneltarsius* from similar-sized *Stockia*. Lower molars of *Stockia* are highly crenulated and m2–3 are distinctive in having mesiodistally very short trigonids with small centrally-placed paraconids. By comparison, *Gunneltarsius* has less crenulated lower molars with longer trigonids and paraconids that are positioned mesial to the metaconid. *Gunneltarsius* also lacks the very broad and rugose m3 talonid with a large hypoconulid lobe and prominent entoconid that is characteristic of *Stockia*. Although upper molars have been attributed to *Stockia* (Lillegraven, 1980), we are uncertain whether these specimens have been correctly attributed to the genus.⁴ Based on the measurements and photographs published in Lillegraven (1980), we believe it is likely that some of the UCMP specimens from the Friars Formation attributed to “*Omomys powayensis*” may instead represent *Gunneltarsius*. The SDNHM upper molars that we here include in the hypodigm of *Gunneltarsius* lack the extreme crenulation seen in lower molars definitively attributed to *Stockia* (Gazin, 1958). It also seems reasonable to expect the M1–2 of *Stockia* to exhibit very small hypocones given the restricted size of its m2–3 trigonids. Most M1–2 specimens of *Gunneltarsius* have hypocones that appear to be too large to occlude well with the small m2–3 trigonids of *Stockia*. Furthermore, M3s attributed to *Gunneltarsius*

do not appear to be sufficiently lingually expanded to occlude well with the very large m3 talonid that is characteristic of *Stockia*.

Gunneltarsius is most similar in morphology to *Omomys* and the largest new omomyoid taxon from the Friars Formation (“*Brontomomys*”; see below). *Gunneltarsius* and *Omomys* share many features, including lingually continuous upper molar cingula and intraspecific variation in the size of the hypocone and pericone on M1–2. Comparisons are further complicated by the considerable variation in p4 morphology represented within the hypodigm of *O. carteri*. Nevertheless, *Gunneltarsius* is most readily distinguished from *Omomys* in the more lingual position of the m2 paraconid, M1–2 with less distal waisting and larger, more inflated conules, and the presence conules on the M3.

Order Primates Linnaeus, 1758
 Semiorder Haplorhini Pocock, 1918
 Infraorder Tarsiiformes? Gregory, 1915
 Superfamily Omomyoidea Trouessart, 1879
 Family Omomyidae Trouessart, 1879
 Subfamily Omomyinae Trouessart, 1879
Brontomomys, gen. nov.
 Type species: *B. cerutti*, sp. nov.

Generic diagnosis Length and width measurements of the upper and lower dentition are absolutely smaller than *Macrotarius montanus*, *Ma. roderi*, *Ma. siegerti*, *Ourayia*, and *Yaquiis*, similar in size to *H. gracilis*, *Macrotarius jepseni*, *Mytonius*, and *Rooneyia*, and larger than *Diablomomys*, *Ekwiymakius*, *Gunneltarsius*, *Omomys*, *Stockia*,

⁴ Lillegraven (1980) figures but does not provide descriptions of these upper molars attributed to “*Omomys powayensis*”. He also notes the possibility that the sample represents more than one taxon, writing “... it cannot be overruled that the 16 specimens (all isolated teeth [of *Stockia*] from two formations) recovered since Gazin’s (1958) study may in reality represent more than a single species...” (p. 190).

Table 3

Measurements of *Gunneltarsius randalli* dentition in millimeters. Length = maximum mesiodistal crown length; Width = maximum buccolingual crown width.

<i>Gunneltarsius randalli</i>			
Specimen number	Position	Length	Width
SDNHM 58778	p3	2.15	1.78
SDNHM 38126	p3	2.12	1.7
SDNHM 38126	p4	2.43	1.89
SDNHM 38126	m1	2.91	2.21
SDNHM 60664	m1	2.8	2.27
SDNHM 56990	m1	2.83	2.27
SDNHM 85940	m1	2.95	2.41
SDNHM 62283	m1	3	2.37
SDNHM 51350	m1	2.87	2.13
SDNHM 49270	m1	2.81	2.19
SDNHM 49270	m2	2.67	2.28
SDNHM 37599	m2	2.4	2.11
SDNHM 56991	m2	2.672	2.18
SDNHM 55109	m2	2.7	2.51
SDNHM 37600	m2	2.64	2.51
SDNHM 60685	m2	2.67	2.2
SDNHM 60665	m2	2.75	2.33
SDNHM 38129	m2	2.72	2.36
SDNHM 87871	m3	3.1	2.08
SDNHM 56992	m3	3.19	2.05
SDNHM 62224	m3	2.9	1.99
SDNHM 55445	m3	3.01	1.99
SDNHM 79804	m3	3.23	2
SDNHM 85941	m3	3.2	1.98
SDNHM 76982	m3	2.87	2.05
SDNHM 40111	m3	3.02	1.91
SDNHM 43814	m3	2.87	1.9
SDNHM 37601	m3		2.17
SDNHM 31648	P3	2.51	2.67
SDNHM 46439	P3	2.81	2.55
SDNHM 38132	P4	2.12	2.86
SDNHM 43097	P4	2.05	2.91
SDNHM 55250	P4	2.16	2.95
SDNHM 55250	M1	2.61	3.58
SDNHM 38135	M1	2.48	3.63
SDNHM 60667	M1	2.55	3.74
SDNHM 43095	M1	2.51	3.54
SDNHM 38134	M1	2.46	3.75
SDNHM 60666	M1	2.55	3.41
SDNHM 31640	M2	2.45	3.68
SDNHM 85942	M2	2.61	4.02
SDNHM 56993	M2	2.65	3.95
SDNHM 76981	M2	2.74	3.93
SDNHM 43094	M2	2.75	4.19
SDNHM 45826	M2	2.87	3.83
SDNHM 37605	M2	2.63	4.04
SDNHM 55250	M3	2.23	3.35
SDNHM 46560	M3	2.16	3.28
SDNHM 55110	M3	2.15	3.32
SDNHM 45827	M3	2.18	3.37
SDNHM 87872	M3	2.06	3.22
SDNHM 38136	M3	2.07	3.15
SDNHM 37453	M3	2.1	3.18
SDNHM 43096	M3	2.28	3.34
SDNHM 38138	M3	1.96	2.91

Utahia, and *Washakius*. Differs from *Diablomomys*, *Ekwiymakius*, *Gunneltarsius*, *Hemiacodon*, *Macrotarsius*, *Mytonius*, *Omomys*, *Ourayia*, *Stockia*, *Utahia*, and *Yaquius* in having an m2-3 paraconid that is positioned lingually and basally fused with the metaconid. Differs from *Diablomomys*, *Ekwiymakius*, *Hemiacodon*, *Macrotarsius*, *Omomys*, *Ourayia*, *Stockia*, and *Yaquius* in having m2-3 paraconids that are similar in size to the metaconid. Differs from *Chumashius*, *Diablomomys*, *Ekwiymakius*, *Omomys*, and *Rooneyia* in having molar occlusal surface crenulation, but differs from *Macrotarsius*, *Stockia*, *Utahia*, and *Washakius* in having less developed molar crenulation. The p4 differs from *Gunneltarsius*, *Macrotarsius*, *Omomys*, *Ourayia*, and *Stockia* in having an entoconid that forms a

small distinct cusp. Differs from *Diablomomys*, *Ekwiymakius*, *Gunneltarsius*, *Hemiacodon*, and *Omomys* in the M1 lacking a waisted distal margin, the M3 lacking a metaconule, and the M1-2 having a mesostyle. Differs from *Diablomomys*, *Ekwiymakius*, *Macrotarsius*, and *Omomys* in having M1-2 paracones that are taller in height relative to the protocone. Differs from *Macrotarsius*, *Omomys*, and *Yaquius* in the P4 lacking a metastyle. Differs from *Ekwiymakius*, *Gunneltarsius*, and *Ourayia* in having a p3 with a lingual cingulid. Differs from *Gunneltarsius*, *Macrotarsius*, and *Omomys* in lacking a p4 postmetacristid. Differs from *Macrotarsius*, *Ourayia*, and *Yaquius* in the presence of a mesiolingual cingulid on the p4. Differs from *Macrotarsius* and *Omomys* in the P3 lacking a metastyle and the M2 lacking a postparaconule and postmetaconule cristae. Differs from *Gunneltarsius* and *Omomys* in the P4 lacking a waisted distal margin. Differs from *Ekwiymakius* and *Macrotarsius* in having a p3 with a buccal cingulid. Differs from *Macrotarsius* and *Ourayia* in the small size of the p4 metaconid. Differs from *Gunneltarsius* and *Macrotarsius* in having a weak m1 postmetacristid. Differs from *Washakius* in having a smaller paraconule and metaconule on M1-2, and in lacking a doubled metaconule. Differs from *Rooneyia* in having smaller M1-2 conules and hypocones. Differs from *Omomys* in lacking a metaconid on the lower p3. Differs from *Stockia* in having a p4 with a metaconid. Differs from *Mytonius* in having a mesiodistally longer p4 with a shorter talonid, an m1 with a more widely-spaced paraconid and protoconid, longer paracristid, and broader trigonid basin, and an m2 with a lingually positioned paraconid. Differs from *Ourayia* in having upper molars with buccal waisting and smaller conules and mesostyles, a P4 and M1 that are buccolingually broader relative to their mesiodistal length, and in an M3 that lacks a lingually continuous cingulum and metaconule.

Etymology From the Greek *brontē* (“thunder”), in reference to the large size of the genus, in combination with *Omomys*, type genus of the Omomyoidea.

Brontomomys cerutti, sp. nov. (Figs. 5–7, Table 4).

Holotype SDNHM 55253, mandibular fragment with p3-m3 and alveoli for i1, i2, c, and p2.

Paratypes SDNHM 56700, maxillary fragment with M2-3; SDNHM 58008, isolated M1.

Hypodigm SDNHM 55252, mandibular fragment with p3-m3 and alveoli for i1, i2, c, and p2; SDNHM 55254, mandibular fragment with p4-m3; SDNHM 55255, mandibular fragment with p4-m1; SDNHM 55258, mandibular fragment with p3-4; SDNHM 60683, isolated c; SDNHM 60681, SDNHM 55819, isolated i1s; SDNHM 60684, isolated p3; SDNHM 55256, SDNHM 46563, SDNHM 60091, isolated m1s; SDNHM 60668, SDNHM 56998, isolated m2s; SDNHM 60680, SDNHM 60670, SDNHM 60669, SDNHM 56999, SDNHM 55785, isolated m3s; SDNHM 58002, SDNHM 58005, SDNHM 58003, SDNHM 58004, isolated P3s; SDNHM 60672, SDNHM 60671, isolated P4s; SDNHM 58009, SDNHM 58010, isolated M1s; SDNHM 58011, SDNHM 55259, isolated M2s; SDNHM 55113, SDNHM 58014, SDNHM 60677, SDNHM 58013, SDNHM 55257, isolated M3s.

Horizon Lower, conglomerate, and upper tongues of the Friars Formation.

Specific diagnosis As for genus.

Etymology Named for SDNHM paleontologist Richard Cerutti, who collected many of the *Brontomomys* specimens described here, including the holotype.

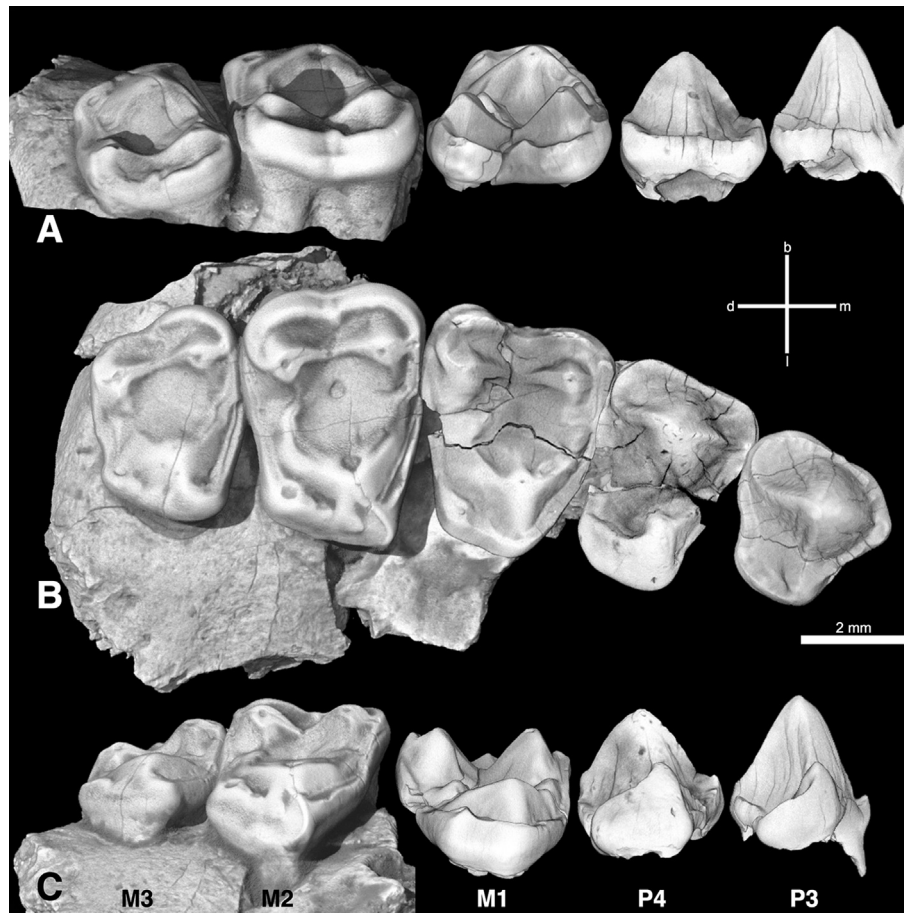


Figure 5. Upper dentition of *Brantomomys cerutti*. A: buccal view, B: occlusal view, C: lingual view. P3: SDNHM 58005; P4: SDNHM 60671, M1: SDNHM 58008; M2-M3: SDNHM 56700. Note that some images have been digitally mirror-imaged to facilitate comparisons.

Description No mandible preserves incisor, canine, or p2 crowns in situ, but single alveoli are present for the i1, i2, c, and p2 in two specimens (SDNHM 55252 and 55253). The largest alveolus is for i1, followed in size by the c alveolus. The smallest alveolus is for i2. Both i1-2 had mesiodistally compressed roots judging from the ovoid shape of their alveoli. The c alveolus is round, and the p2 alveolus is variably round or ovoid in shape. There is no evidence of a p1 alveolus in any specimen. One isolated i1 (SDNHM 60681) has a lanceolate crown with a pronounced lingual crest and mesial cingulid. The i1 crown is asymmetrical in lateral view, with the most projecting labial portion of the tooth located closer to the apex of the crown's single cusp than the most projecting lingual portion of the tooth near the terminus of the mesial cingulum. SDNHM 60681 has a large root with dimensions that closely match the i1 alveolus of the holotype. When these specimens are virtually combined (Fig. 7), the i1 is strongly procumbent as in *Macrotarius jepseni*, which is reflected in the strong anterior inclination of the i1 alveolus. The i1 crown is large and comparable in size to the p3 crown. The p3 of *Brantomomys* is moderately long, with the mesiodistal length greater than half the length of the m1. The p3 protoconid is taller in height relative to that of the p4 and m1. The p3 has weak lingual, buccal, and mesiobuccal cingulids. The p3 paraconid is variable in size. The p3 lacks a metaconid, has a small cusped hypoconid, and a variably sized entoconid. The p4 is shorter in mesiodistal length than the m1. The p4 protoconid is taller than that of the m1. The p4 paraconid is variable, and may be cingulid-like or absent entirely. The p4 metaconid is a small, distinct cusp that is positioned slightly more distally than the protoconid. The p4

lacks a lingual cingulid, and has a mesiolingual, buccal, and mesiobuccal cingulid. The p4 hypoconid and entoconid are small cusps. The lower premolar crowns of *Brantomomys* are slightly overlapping. The m1 paraconid is a conical cusp that is positioned slightly more buccally than the metaconid. The m1 trigonid is lingually open. The m3 hypoconulid lobe is large and positioned near the buccolingual midline. The m1-2 buccal and mesiobuccal cingulids are strong. The lower molars lack a lingual or mesiolingual cingulid. The m2-3 paraconids are positioned lingually and are basally fused to the metaconid. The P3 of *Brantomomys* is moderate in size but smaller than the P4. The P3 paracone is taller in height than the P4 paracone. The P3-4 metacone and hypocone are absent and the protocone is present as a small cusp. The P3-4 lack a metastyle but have a small cusped parastyle. The P3-4 buccal, mesial, and distal cingula are all strong, while the lingual cingulum is absent. The P3 has waisted mesial and distal margins, but the P4 lacks a comparable waisting. The M1 is slightly smaller than the M2. The M1-2 hypocones are present and positioned distolingual to the protocones. The M1 has a short postprotocingulum that splits from the postprotocrista between the hypocone and metaconule and terminates before reaching the distal cingulum. The presence of a pericone is variable on the M1 of *Brantomomys*; some specimens lack a pericone, while other specimens have a small, distinct cusp. The M1-2 paraconule and metaconule are small. The M1-2 lack a waisted distal margin. The M1-2 buccal, mesial, and distal cingula are strong. The M1-2 parastyle and metastyle are present as small cusps. The M1-2 have a narrow styler shelf with small but distinct mesostyles. The M2 lacks a cusped pericone. The M3 is

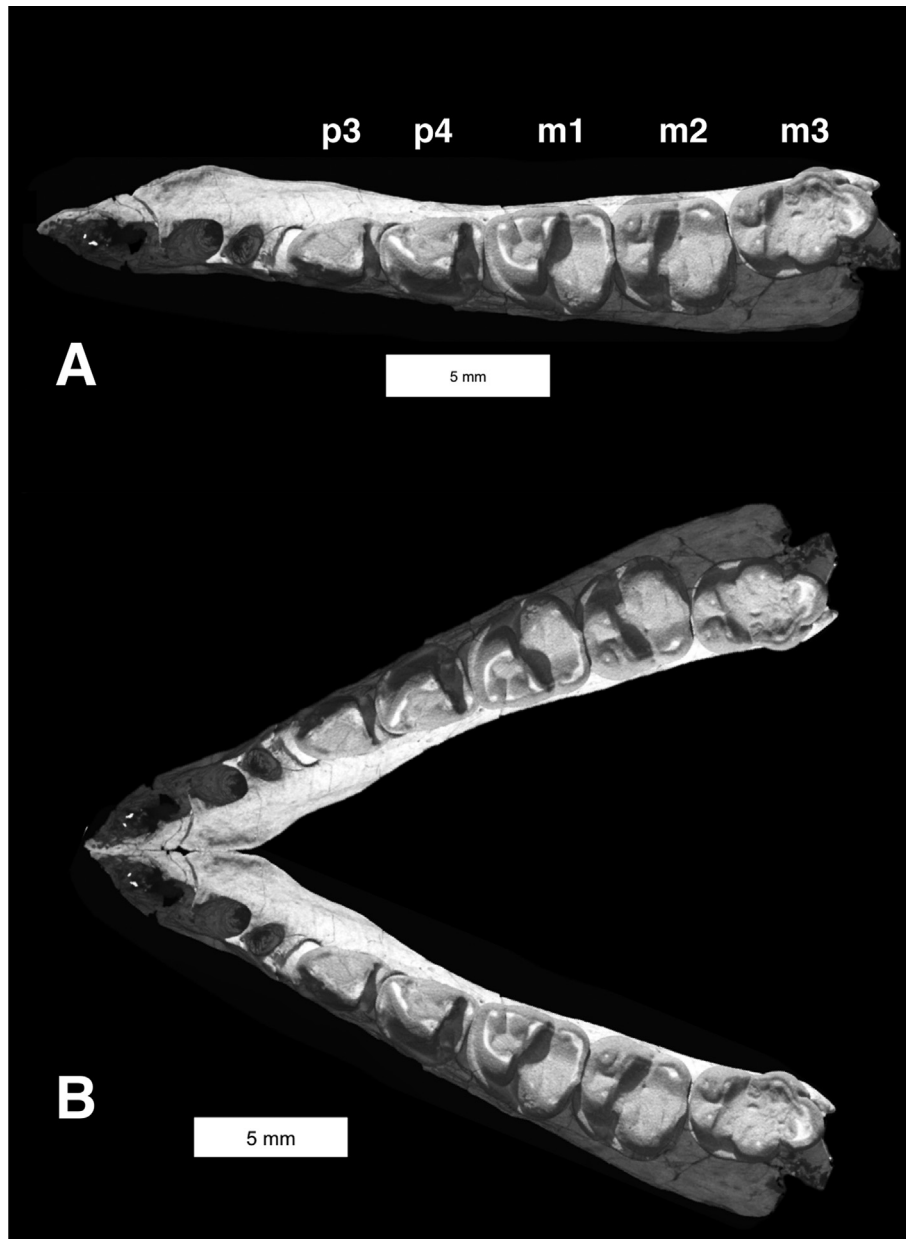


Figure 6. Occlusal view of *Brontomomys cerutti* holotype. A: SDNHM 55253, mandibular specimen. B: mirroring the mandible allows reconstruction of the dental arcade.

slightly smaller than the M1 and M2. The M3 hypocone is variable; in some specimens this feature is absent, and in others the M3 hypocone is present as a small cusp. The M3 has a weak post-protocingulum. Upper molars have lingual cingula that are variable, both in terms of presence or absence and whether (if present) they are continuous or discontinuous. Upper and lower molar occlusal surfaces are moderately crenulated.

Discussion With dental dimensions similar to *Macrotarsius jepsoni*, *Brontomomys* is noteworthy for its large size. *Brontomomys* may be readily discriminated from the large Southern California omomyoid *Yaquioides* in having a p3-4 that are buccolingually narrower relative to their mesiodistal width, a p4 with a smaller paraconid, and an m2 with a closely approximated paraconid and metaconid. Among known omomyoid taxa, *Brontomomys* is most similar in morphology to *Gunneltarsius*, *Macrotarsius*, and *Ourayia*. All four taxa have p3 protoconids that are taller in height relative to

the p4 or m1. They also share upper and lower molar occlusal surface crenulation. *Brontomomys* shares with *Macrotarsius* and *Ourayia* broad upper molars with a distinct styler shelf, including a mesostyle on the M1-2. The lower premolars of *Brontomomys*, *Macrotarsius*, and *Ourayia* also show similarities in occlusal profile and degree of cingulid development.

Despite these similarities, *Brontomomys* differs from the smaller Friars Formation genus *Gunneltarsius* in having a p4 with a proportionally larger metaconid, proportionally smaller m2-3 trigonid basins, and upper molars with broad styler shelves and mesostyles. *Brontomomys* may be readily distinguished from *Macrotarsius* in the morphology of the p4. In *Macrotarsius macrorhysis*, *Macrotarsius montanus*, *Macrotarsius roederi*, *Macrotarsius siegerti*, and to a lesser extent *Macrotarsius jepsoni*, the p4 has a larger, cusped paraconid and a mesiodistal length that is more similar to its buccolingual width. By comparison, the p4 of *Brontomomys* has a

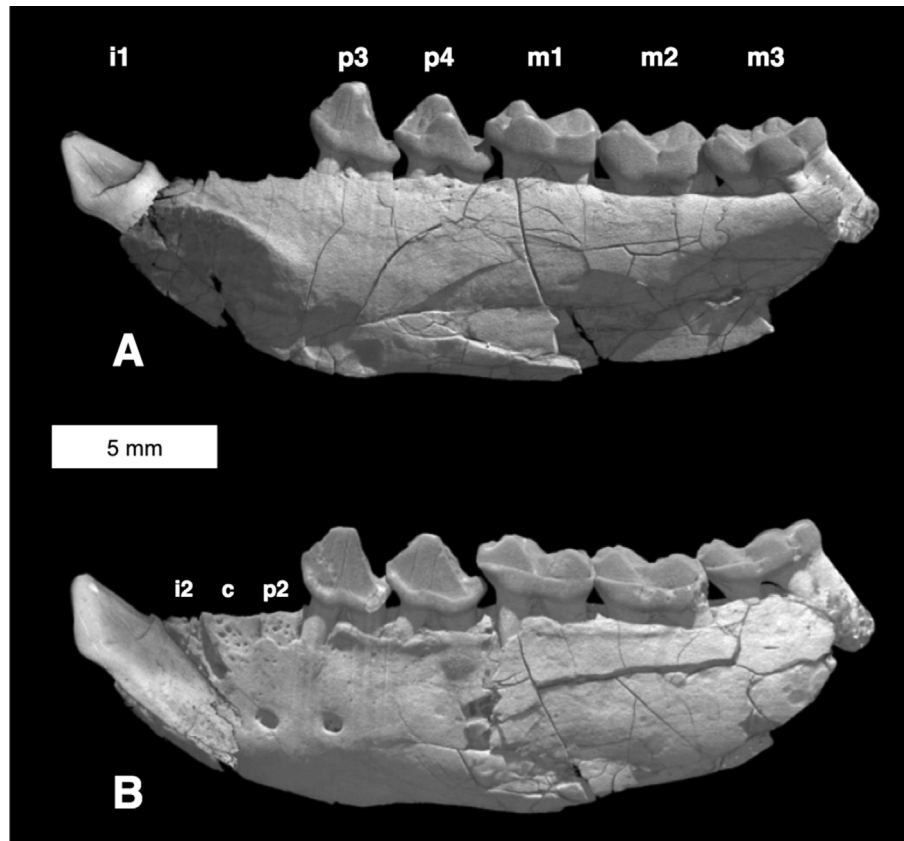


Figure 7. Lateral views of holotype specimen of *Brontomomys cerutti*, SDNHM 55253. A: lingual view, B: buccal view. The mandible has been virtually combined with an isolated incisor (SDNHM 60681). SDNHM 60681 has a large root with dimensions that closely match the i1 alveolus of the holotype. Note that image A has been digitally mirrored.

low, crestiform paraconid and is much longer mesiodistally than it is buccolingually. In these respects, the p4 of *Brontomomys* closely resembles that of *Ourayia*. Indeed, the lower dentitions of *Brontomomys* and *Ourayia* are very similar in morphology, differing most prominently in the structure of the m2-3 trigonids. In *Brontomomys*, the paraconid and metaconid are similar in size on m2-3, and the paraconid is lingually positioned mesial to the metaconid. By contrast, in *Ourayia* the paraconid is more buccally positioned and is smaller than the metaconid on m2-3. All species of *Macrotarsius* differ from both *Brontomomys* and *Ourayia* in having m2-3 paraconids that are more widely spaced from the metaconid. *Brontomomys* and *Ourayia* are more easily discriminated by the morphology of the P4-M3. In *Ourayia* (e.g., CM 80200), the protocone and postprotocrista are positioned on the lingual margin of the P4 and there is a broad fossa distal to the mesiolingually positioned protocone. By contrast, in *Brontomomys* the P4 protocone and postprotocrista are more buccally positioned and the fossa distolingual to the protocone is much smaller. Furthermore, the P4 and M1 of *Ourayia* have buccolingual widths that are more similar to their mesiodistal lengths. In *Brontomomys* the P4 and M1 are proportionally broader in mesiodistal width, lending these teeth a more rectangular and less squared occlusal profile. *Brontomomys* also differs from *Ourayia* in having buccally waisted upper molars, less well developed upper molar conules and mesostyles, and in lacking an M3 metaconule entirely.

4.2. Body mass

Figure 8 illustrates the comparative dimensions of upper and lower molars of *Ekwiymakius*, *Gunneltarsius*, and *Brontomomys*. According to the prosimian regression of Conroy (1987), body

masses of *Ekwiymakius*, *Gunneltarsius*, and *Brontomomys* are estimated to have been 113–125 g, 275–303 g, and 719–796 g, respectively (Table 1). Conroy's (1987) all-primate regression yields larger estimates of 124–138 g, 330–366 g, and 958–1061 g for *Ekwiymakius*, *Gunneltarsius*, and *Brontomomys*, respectively. These estimates for *Ekwiymakius* and *Gunneltarsius* are broadly comparable to that of a range of North American anaptomorphines and omomyines (Fleagle, 2013). However, the estimated body mass of *Brontomomys* is large compared to most omomyoids (Fleagle, 2013), with dental dimensions most similar to *H. gracilis*, *Mytonius hopsoni*, and *Macrotarsius jepseni* among North American taxa.

4.3. Phylogenetic analyses

The parsimony analysis of the Ni matrix produced 32 equally parsimonious trees. Of the 510 total characters included in the Ni matrix, 181 characters are constant and 70 variable characters are parsimony-uninformative, leaving 259 parsimony-informative characters. The 50% majority-rule tree (Fig. 9A) shows *Gunneltarsius* and *Brontomomys* as sister taxa. Basal to *Gunneltarsius* and *Brontomomys* is *Yaqui*, followed by *Diablomomys*. These four taxa comprise the sister clade to *Stockia*, *Utahia*, and *Ourayia*. *Ekwiymakius* is basal to those seven taxa, followed by *Macrotarsius*, *Ekgmowechashala*, and *Omomys* + *Chumashius*. However, bootstrap support values are generally low within this group, and the only clades with >50% bootstrap support are *Chumashius* + *Omomys* and *Ma. montanus* + *Ma. siegerti*. Furthermore, some taxa that are typically considered omomyines (e.g., *Hemiacodon*, *Washakius*, and *Dyseolemur*; Tornow, 2008) group with an assemblage of anaptomorphine and microchoerine species.

Table 4

Measurements of *Brontomomys cerutti* dentition in millimeters. Length = maximum mesiodistal crown length; Width = maximum buccolingual crown width.

<i>Brontomomys cerutti</i>			
Specimen number	Position	Length	Width
SDNHM 55252	p3	2.97	2.04
SDNHM 55253	p3	2.98	2.09
SDNHM 55258	p3	3.06	2.09
SDNHM 55252	p4	3.28	2.5
SDNHM 55253	p4	3.03	2.52
SDNHM 55258	p4	3.47	2.48
SDNHM 55254	p4	3.51	2.46
SDNHM 55255	p4	3.09	2.3
SDNHM 55252	m1	3.71	3.09
SDNHM 55253	m1	3.61	3.17
SDNHM 55254	m1	3.98	2.92
SDNHM 55255	m1	3.94	3.01
SDNHM 55256	m1	3.82	2.95
SDNHM 46563	m1	3.89	2.86
SDNHM 60091	m1	4.11	3.19
SDNHM 55252	m2	3.57	3.26
SDNHM 55253	m2	3.38	3.23
SDNHM 55254	m2	3.82	3.48
SDNHM 60668	m2	3.42	3.4
SDNHM 56998	m2	3.62	3.12
SDNHM 55252	m3	4.55	2.86
SDNHM 55253	m3	4.19	3.01
SDNHM 55254	m3	4.57	3.05
SDNHM 60680	m3		2.7
SDNHM 60670	m3	3.89	2.84
SDNHM 60669	m3	3.77	2.47
SDNHM 56999	m3	3.75	2.77
SDNHM 55785	m3	3.98	3.02
SDNHM 58002	P3	2.98	2.85
SDNHM 58005	P3	3.33	3.3
SDNHM 58004	P3	3.31	3.06
SDNHM 60673	P4	2.79	
SDNHM 56194	P4	2.46	3.36
SDNHM 58772	P4	2.42	
SDNHM 60671	P4	2.86	4
SDNHM 60672	P4	2.56	3.44
SDNHM 60674	M1	3.45	4.32
SDNHM 60676	M1	3.26	4.87
SDNHM 58008	M1	3.57	4.43
SDNHM 58009	M1	3.24	4.47
SDNHM 58010	M2	3.35	4.78
SDNHM 58011	M2	3.72	4.89
SDNHM 55259	M2	3.17	4.68
SDNHM 56700	M2	3.25	5.01
SDNHM 56700	M3	3.04	4.04
SDNHM 55113	M3	2.91	4.55
SDNHM 58014	M3	2.7	4.12
SDNHM 60677	M3	2.99	4.52
SDNHM 58013	M3	2.62	4.2
SDNHM 55257	M3	2.99	4.32

The Bayesian analysis of the Ni matrix resulted in two runs of 3,500,000 generations with average standard deviation of split frequencies of 0.03. Run one resulted in 0.54 proportions of successful state exchanges between chains, run two resulted in 0.55. The majority-rule consensus tree (Fig. 9B) shows *Gunneltarsius* and *Brontomomys* as sister taxa, with *Yaquiuis* and *Diablomomys* as successive sister taxa to this clade. This clade of four is sister to a clade including *Stockia*, *Utahia*, *Ourayia*, and *Macrotarsius*. Basal to this group is *Ekwiymakius*, followed successively by *Omomys* and *Chumashius*. Bootstrap support for this topology is somewhat greater than that of the parsimony analysis, with the entire clade receiving 88% support. Within the larger clade, a sister–taxon relationship between *Gunneltarsius* and *Brontomomys* received 51% support, and the clade comprised of *Ekwiymakius*, *Gunneltarsius*, *Brontomomys*, *Yaquiuis*, *Diablomomys*, *Stockia*, *Utahia*, *Ourayia*, and *Macrotarsius* received 81% bootstrap support. However, as

in the parsimony analysis, several omomyine taxa including *Hemiacodon* are distributed throughout a clade of anaptomorphines and microchoerines.

The parsimony analysis of the Tornow matrix produced 11 equally parsimonious trees. Of the 100 total characters included in the Tornow matrix, one character is constant and seven variable characters are parsimony-uninformative, leaving 92 parsimony-informative characters. The 50% majority-rule tree (Fig. 10A) recovers *Brontomomys* as the sister taxon to *Utahia*, with *Ourayia* basal to this clade. *Ekwiymakius* and *Gunneltarsius* are shown as sister taxa, and together form a clade with *Brontomomys*, *Utahia*, and *Ourayia*. *Omomys*, *Macrotarsius*, and *Hemiacodon* are successive stem members of the clade that includes *Brontomomys*, *Ekwiymakius*, and *Gunneltarsius*. However, bootstrap support for this topology is very low, with values for all omomyine nodes below 50%.

The Bayesian analysis of the Tornow matrix resulted in two runs of 2,000,000 generations with average standard deviation of split frequencies of 0.01. Run one resulted in 0.79 proportions of successful state exchanges between chains, run two resulted in 0.77. The majority-rule consensus tree (Fig. 10B) again shows *Brontomomys* as the sister taxon to *Utahia*. *Brontomomys* and *Utahia* in turn form a clade with *Ourayia* and *O. carteri*. *Gunneltarsius* and *Ekwiymakius* are successive stem members of the clade that includes *Brontomomys*, *Utahia*, *Ourayia*, *Omomys*, *Macrotarsius*, *Hemiacodon*, *Washakius*, and *Shoshonius*. Bootstrap support of this topology is greater than that for the parsimony-based tree, with the clade that includes *Brontomomys*, *Gunneltarsius*, and *Ekwiymakius* receiving 90% support.

5. Discussion

Here we document the presence of three new omomyoid genera from the early Uintan of Southern California. These new taxa represent at least part of the SDNHM Friars Formation omomyoid sample that Walsh (1996) provisionally referred to *Omomys* and *Ourayia*.⁵ With the addition of these new taxa, the fossil primate community represented in the Friars Formation of San Diego County now includes at least six primate genera: the adapiform *Hesperolemur* (or *Cantius*) and the omomyoids *Brontomomys*, *Ekwiymakius*, *Gunneltarsius*, *Stockia*, and *Washakius*.⁶ With the exception of *Washakius*, all of these primate genera are currently known from only the Friars Formation (Walsh, 1996).

5.1. Phylogenetic results

In undertaking our phylogenetic analyses, our goal was not to resolve omomyoid phylogenetic relationships more broadly, but instead to provide a hypothesis of the phylogenetic affinities of the new San Diego taxa. We chose to analyze the Ni et al. (2016) matrix based upon its large number of included taxa, large number of dental characters, and recent publication date. Although the Tornow (2008) matrix has fewer characters and included taxa, we

⁵ It is not yet clear how the new taxa described here relate to the University of California Museum of Paleontology (UCMP) specimens from the Friars Formation that Lillegraven (1980) referred to “*Macrotarsius* sp. near *M. jepseni*” because we have not yet examined that material.

⁶ Although a detailed description of additional specimens is beyond the scope of the current paper, the SDNHM Friars Formation primate sample also includes isolated omomyoid teeth similar in morphology to *Trogolemur* and comparable in size to *T. fragilis*. Also included are the m2 (SDNHM 4251-6226) and m3 (SDNHM 4251-6227) of a large omomyoid from a single individual (based on matching interproximal contact facets). In both size and morphology, these two lower molars closely resemble *Ourayia uintensis*.

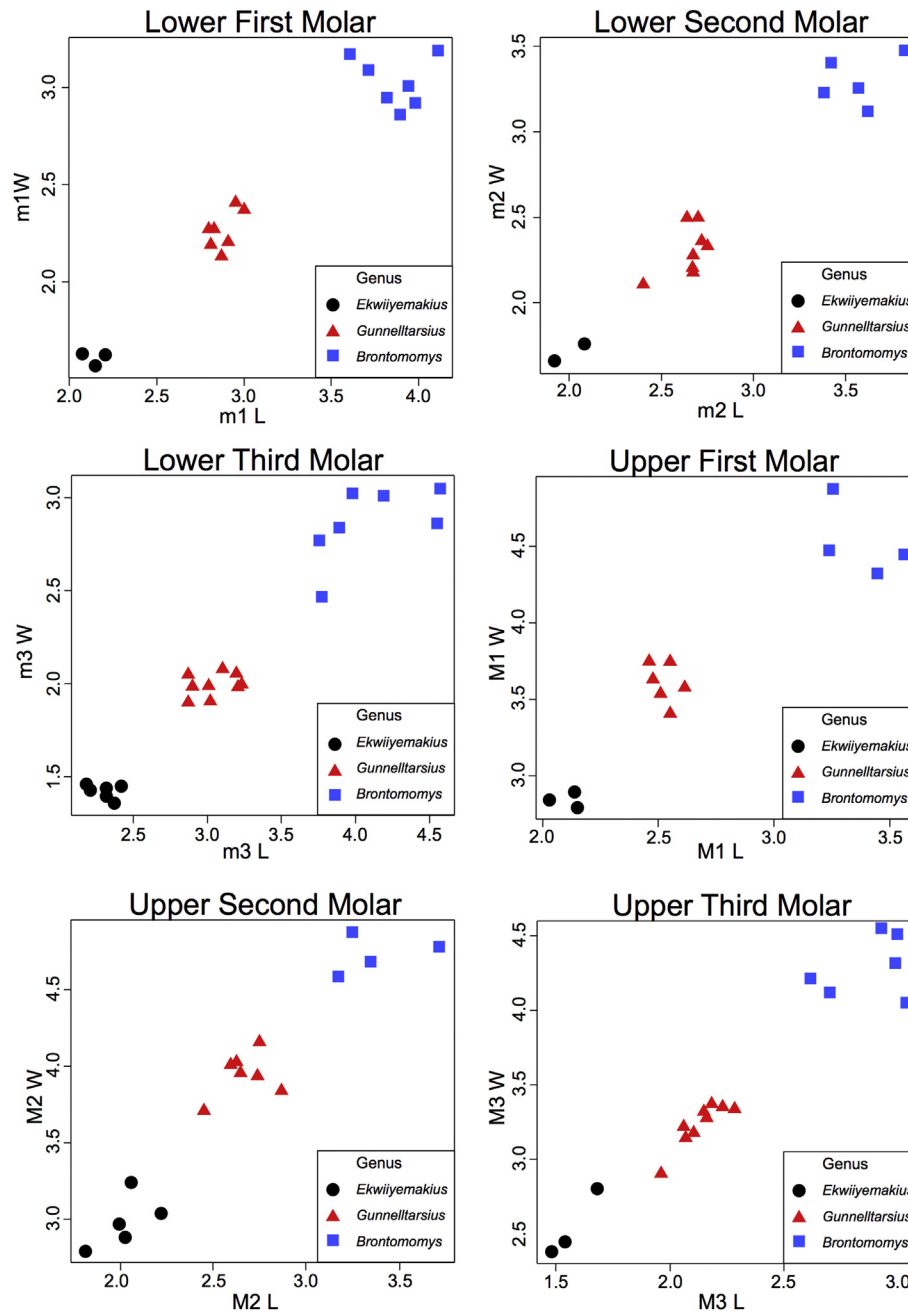


Figure 8. Length x Width (mm) dimensions of the three new taxa.

chose to analyze this dataset in parallel because it was designed specifically to study the phylogenetic relationships of North American omomyoids. We further chose to analyze the two character-taxon matrices using both parsimony and Bayesian tree building methods. For decades, parsimony has been widely used to reconstruct phylogeny from standard phenotypic data (Wright and Hillis, 2014). However, one potential problem with parsimony analyses is that only parsimony-informative characters are used in the analysis. The distribution of these parsimony-informative characters does not necessarily reflect the true distribution of all the observable characters, therefore creating a sampling bias (Wright and Hillis, 2014). This bias leads to poor estimates of character rate evolution and inflated estimates of character change. Lewis (2001) introduced versions of the Bayesian Mk model that corrects for biases in character evolution. This likelihood method takes

rate heterogeneity between sites into account, whereas the default for parsimony methods is for character change to be weighted equally (Wright and Hillis, 2014). Accounting for rate heterogeneity is argued to more accurately reflect evolutionary processes as sampled characters within datasets may evolve via differing rates, developmental processes, and modes of evolution (Clarke and Middleton, 2008; Wagner, 2012).

The four phylogenetic analyses presented here yield majority-rule consensus trees that differ substantially in their topology (Figs. 9 and 10). This result is not surprising given the fact that we analyzed two matrices with very different characters and ingroup taxa, and analyses of large morphological character-taxon matrices have thus far produced little consensus regarding omomyoid systematics (e.g., Tornow, 2008; Ni et al., 2016). In both the parsimony and Bayesian analyses of the Ni matrix (Fig. 9), *Gunnellarsius* and

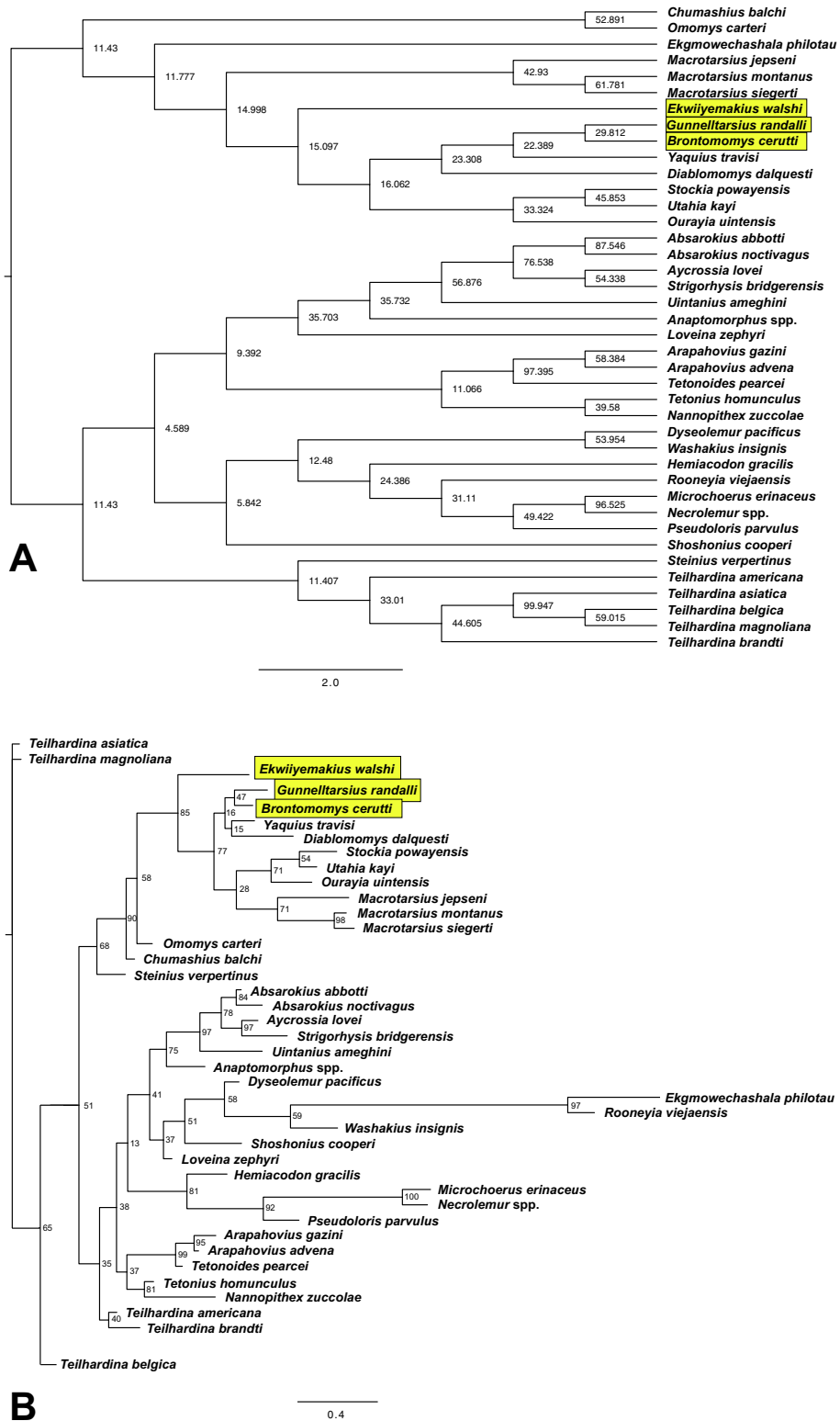
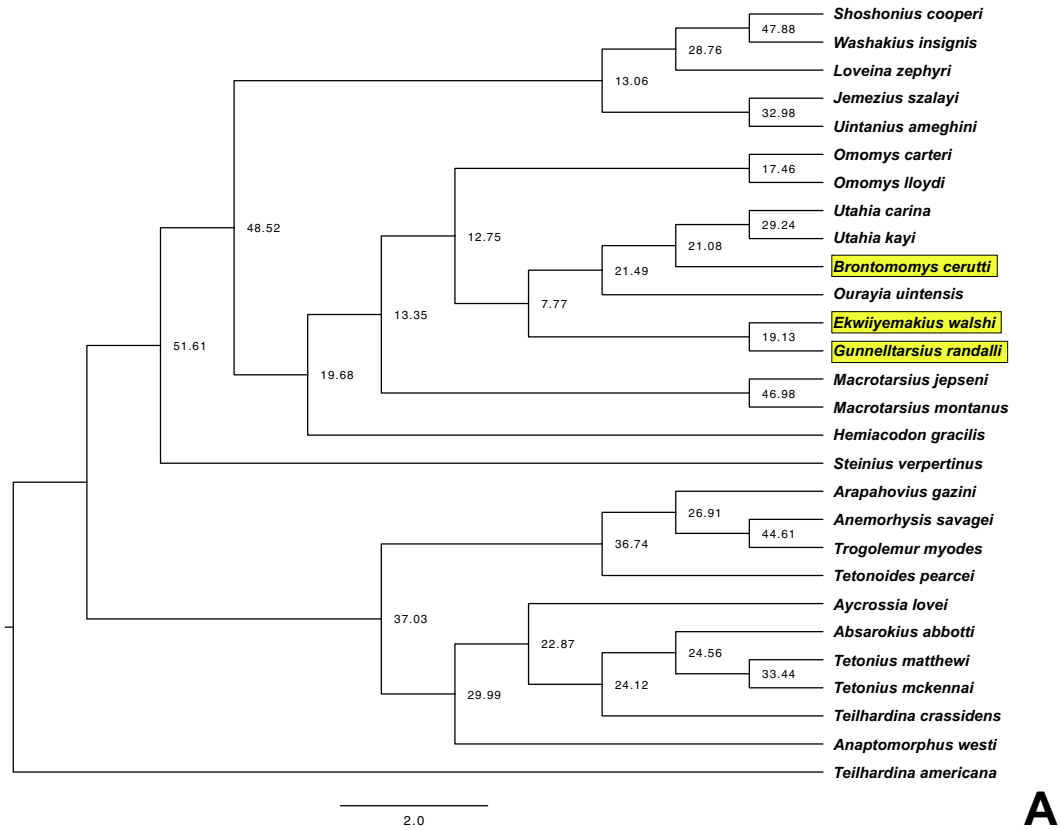


Figure 9. Phylogenetic trees using the Ni et al. (2016) character matrix. A: Phylogenetic majority-rule tree produced through parsimony analysis using PAUP* and the Ni et al. (2016) character-taxon matrix, plus addition of new taxa. Values at nodes represent bootstrap support. B: Phylogenetic majority-rule tree produced through Bayesian analysis using MrBayes and the Ni et al. (2016) character-taxon matrix, plus addition of new taxa described here. Values at nodes represent posterior probability.

Brontomomys are recovered as sister taxa within a larger clade that includes *Yaquius*, *Diablomomys*, *Stockia*, *Utahia*, and *Ourrayia*. *Ekwiymakius* is recovered as basal to this group in both analyses of the Ni matrix. *Macrotarsius* is either sister taxon to this clade

including *Gunneltarsius*, *Brontomomys*, and *Ekwiymakius* (Ni parsimony: Fig. 9A), or falls within the clade as sister taxon to *Stockia*, *Utahia*, and *Ourrayia* (Ni Bayesian: Fig. 9B). By contrast, in both the parsimony and Bayesian analyses of the Tornow matrix



A



B

Figure 10. Phylogenetic trees using the [Tornow \(2008\)](#) character matrix. A: Phylogenetic majority-rule tree produced through parsimony analysis using PAUP* and the [Tornow \(2008\)](#) character-taxon matrix, plus addition of new taxa. Values at nodes represent bootstrap support. B: Phylogenetic majority-rule tree produced through Bayesian analysis using MrBayes and the [Tornow \(2008\)](#) character-taxon matrix, plus addition of new taxa described here. Values at nodes represent posterior probability.

(Fig. 10), *Brontomomys* is recovered as the sister taxon to *Utahia* in a clade that also includes *Ourayia*. *Gunneltarsius* and *Ekwiymakius* are either sister taxa (Tornow parsimony: Fig. 10A) or successive basal members of a clade including *Shoshonius*, *Washakius*, *Hemiacodon*, *Macrotarsius*, *Omomys*, *Brontomomys*, *Utahia*, and *Ourayia* (Tornow Bayesian: Fig. 10B). The inconsistency of these results according to (1) the choice of character-taxon matrix and (2) the use of parsimony versus Bayesian tree building methods leads us to have little confidence in preferring one specific topology over another. Nevertheless, all four analyses are fairly consistent in grouping the three new San Diego taxa with a larger assemblage of omomyoids that includes *Macrotarsius*, *Omomys*, *Ourayia*, and *Utahia*. These results reinforce our initial conclusion that *Brontomomys*, *Gunneltarsius*, and *Ekwiymakius* share morphological affinities with taxa that are often classified within the subfamily Omomyinae (Tornow, 2008; Fleagle, 2013). Omomyine affinities are further supported by the two Bayesian analyses, which provide strong bootstrap support for linking the three new San Diego genera with *Chumashius*, *Diablomomys*, *Macrotarsius*, *Omomys*, *Ourayia*, *Stockia*, *Utahia*, and *Yaquius* (Fig. 9B) or with *Hemiacodon*, *Macrotarsius*, *Omomys*, *Ourayia*, *Shoshonius*, *Utahia*, and *Washakius* (Fig. 10B). Despite differences in tree topology, congruence between analyses provides strong support for the omomyine status of each of these three new genera.

5.2. Faunal dynamics and paleobiogeography

Southern California Previous authors have suggested that mammalian faunas from Southern California demonstrate a shift toward greater provincialism from the early to the late Uintan (Golz and Lillegraven, 1977; Lillegraven, 1980; Walsh, 1991, 1996). This conclusion was based partly on the primates that have been identified from the early Uintan of Southern California, with both Lillegraven (1980) and Walsh (1996) recognizing the presence of genera (e.g., *Omomys* and *Washakius*) that are well known from Bridgerian faunas in the Western Interior. The presence of these more cosmopolitan primate taxa in the early Uintan contrasted with the presence of endemic primate genera like *Dyseolemur*, *Chumashius*, and *Yaquius* in late Uintan and Duchesnean faunas from Southern California (Walsh, 1996; Robinson et al., 2004). Major tectonic events along the Pacific coast of North America have been proposed as one cause of this increased endemism during the late Uintan (Lillegraven, 1980).

This analysis suggests that the primate community from the Friars Formations was more provincial in character than has been previously appreciated. Like *Hesperolemur* (if valid) and *Stockia*, the three new omomyine genera described here are currently known from only the Friars Formation and may represent taxa that are endemic to Southern California. The species *W. woodringi* is also unknown outside of the early Uintan of Southern California. Furthermore, although *Omomys* occurs in early Uintan assemblages in the Western Interior (Kelly and Murphey, 2015) and Trans-Pecos Texas (West, 1982), claims that *Omomys* is present in the early Uintan of Southern California should be treated with caution. Lillegraven (1980) identified *Omomys* as present in the Friars Formation in part because he believed that *Stockia* is a junior synonym of *Omomys*. If we are correct that Lillegraven's (1980) collection of isolated teeth that he attributed to "*Omomys powayensis*" includes specimens of *Gunneltarsius*, then the acknowledged heterogeneity of this sample may have obscured the distinctive features of the lower molars that are diagnostic of the genus *Stockia* (Gazin, 1958). Walsh's (1996) identification of *Omomys* from the Friars Formation was provisional, and we believe it is likely that all of the specimens on which this assessment was based can be accommodated within *Gunneltarsius* and *Ekwiymakius*. Accordingly, we are not aware of

any convincing evidence that *Omomys* was present in the Uintan of Southern California. These considerations suggest that the Friars Formation primate fauna had few cosmopolitan taxa and was instead dominated by regional endemics (e.g., *Brontomomys*, *Gunneltarsius*, *Ekwiymakius*, *Stockia*, and possibly *Hesperolemur*).

North America The addition of *Ekwiymakius*, *Gunneltarsius*, and *Brontomomys* to the known North American omomyine diversity allows for a better understanding of primate richness in the Uintan. Previous workers, looking mainly to the Rocky Mountain basins, suggested that primate richness declined through the Uintan (Gunnell and Bartels, 1999). For example, Rasmussen et al. (1999:407) noted that "one of several important faunal contrasts distinguishing the Uintan NALMA from the earlier Wasatchian and Bridgerian NALMAs is the great reduction in primate richness and the complete absence of the familiar, large bodied notharctines in the Rocky Mountain Region". This interpretation of primate decline stems mainly from more than 20 Bridgerian primate taxa named from the southern Green River Basin that virtually disappear by the Uintan (Williams and Kirk, 2008).

More recent research shows that while primate richness declined in the greater Green River Basin during the Uintan, primate richness increased during the Uintan in other locations in North America (Simons, 1961; Lillegraven, 1980; Honey, 1990; Westgate, 1990; Walsh, 1991, 1996; Gunnell, 1995; Rasmussen et al., 1995; Kirk and Williams, 2011; Williams and Kirk, 2008; Gunnell et al., 2009; Murphey and Dunn, 2009; Murphey et al., 2017). The available data do support the conclusion that adapiform and anaptomorphine richness declined precipitously from the Bridgerian to the Uintan. By comparison, omomyine richness remained relatively stable through the middle Eocene. Williams and Kirk (2008) noted that the Bridgerian records 14 omomyine species and the Uintan records 15. The work presented here increases the number of Uintan omomyines from 15 to 18, and further highlights the relevance of fieldwork outside the Rocky Mountain interior for understanding of North American primate richness during the middle Eocene.

6. Conclusions

Here we describe three new genera of early Uintan primates from the Friars Formation of San Diego County, California: *Brontomomys*, *Gunneltarsius*, and *Ekwiymakius*. Although interpretations of omomyoid phylogenetic relationships vary according to character-taxon matrix and tree-building methods, the available evidence suggests that the three new genera form a clade with the omomyine primates *Utahia*, *Ourayia*, *Omomys*, and *Macrotarsius*. Like the previously described taxa *Hesperolemur* and *Stockia*, *Brontomomys*, *Gunneltarsius*, and *Ekwiymakius* are currently known from only the Friars Formation. The addition of three new endemic taxa suggests that early Uintan primate faunas from Southern California may be more provincial than has previously been appreciated.

Acknowledgments

This paper would not have been possible without the generous assistance of Kesler Randall and Thomas Deméré at the SDNHM. Special thanks are also due to Liza Shapiro, who provided comments on an earlier version of this manuscript, to Beth Townsend, who kindly allowed us to examine unpublished specimens from the Uinta Basin, to Tab Rasmussen, who provided casts of undescribed *Ourayia* specimens from the Uinta Basin, and to Simon Scarpetta, Addison Kemp, David Hillis, David Cannatella, Meaghan Wetherell, Kelly Thomson and Joshua Lively for assistance with phylogenetic analyses. Additional casts of fossil specimens were provided by

Chris Beard, Chris Bell, Doug Boyer, Rachel Dunn, Gregg Gunnell, Amy Henrici, Samuel McLeod, Paul Murphey, Ken Rose, Bill Sanders, Alan Tabrum, and Blythe Williams. Assistance with CT scanning and digital rendering was provided by Matt Colbert, Jessie Maisano, and the staff of the UT High-Resolution X-ray Computed Tomography Facility. Doug Boyer and Mackenzie Shepard provided assistance in making micro CT files available on Morphosource. This paper was also greatly improved by revisions suggested by Beth Townsend and two anonymous reviewers. This research was supported by a National Science Foundation Graduate Research Fellowship (DGE-1610403). Any opinions, findings, and conclusions or recommendations expressed in this material are those of the authors and do not necessarily reflect the views of the National Science Foundation.

Supplementary Online Material

Supplementary online material related to this article can be found at <https://doi.org/10.1016/j.jhevol.2017.03.013>.

References

- Beard, K.C., 1987. *Jemezium*, a new omomyid primate from the early Eocene of northwestern New Mexico. *Journal of Human Evolution* 16, 457–468.
- Bottjer, D., Lund, S., Powers, J., Steele, M., Squires, R., 1991. Magnetostratigraphy of Paleogene strata in San Diego and the Simi Valley, southern California. In: Abbott, P.L., May, J.A. (Eds.), *Eocene Geologic History San Diego Region*. Pacific Section, SEPM, pp. 115–124.
- Clarke, J., Middleton, K., 2008. Mosaicism, modules, and the evolution of birds: results from a Bayesian approach to the study of morphological evolution using discrete character data. *Systematic Biology* 57, 185–201.
- Conroy, G.C., 1987. Problems of body-weight estimation in fossil primates. *International Journal of Primatology* 8, 115–137.
- Cuozzo, F.P., 2008. Using extant patterns of dental variation to identify species in the primate fossil record: a case study of middle Eocene *Omomyx* from the Bridger Basin, southwestern Wyoming. *Primates* 49, 101–115.
- Fleagle, J.G., 2013. Fossil Prosimians. In: *Primate Adaptation and Evolution*, second ed. Academic Press, San Diego, pp. 330–398.
- Flynn, J., 1986. Correlation and geochronology of middle Eocene strata from the western United States. *Palaeogeography, Palaeoclimatology, Palaeoecology* 55(2–4), 335–406.
- Gazin, C.L., 1958. A review of the Middle and Upper Eocene primates of North America. *Smithsonian Miscellaneous Collections* 136, 1–131.
- Golz, D.J., Lillegraven, J.A., 1977. Summary of known occurrences of terrestrial vertebrates from Eocene strata of southern California. *Contributions to Geology, University of Wyoming* 15, 43–64.
- Gunnell, G., Bartels, W., 1999. Middle Eocene vertebrates from the Uinta Basin, Utah, and their relationship with faunas from the southern Green River Basin. *Utah State Geological Survey, Wyoming. Vertebrate Paleontology of Utah*. Salt Lake, pp. 429–442.
- Gunnell, G.F., 1995. New Notharctine (Primates, Adapiformes) skull from the Uinta (Middle Eocene) of San Diego County, California. *American Journal of Physical Anthropology* 98, 447–470.
- Gunnell, G.F., Murphey, P.C., Stucky, R.K., Townsend, K.E.B., Robinson, P., Zonneveld, J.-P., Bartels, W.S., 2009. Biostratigraphy and biochronology of the latest Wasatchian, Bridgerian, and Uintan North American Land Mammal “Ages.” *Papers on Geology, Vertebrate Paleontology, and Biostratigraphy in Honor of Michael O. Woodburne*, pp. 279–330.
- Honey, J.G., 1990. New Washakiini primates (Omomyidae) from the Eocene of Wyoming and Colorado, and comments on the evolution of the Washakiini. *Journal of Vertebrate Paleontology* 10, 206–221.
- Kelly, T.S., Murphey, P.C., 2015. Mammals from the earliest Uintan (middle Eocene) Turtle Bluff Member, Bridger Formation, southwestern Wyoming, USA, Part 1: Primates and Rodentia. *Palaeontologia Electronica*. <https://doi.org/10.26879/586.19.2.26A>: 1–55.
- Kennedy, M.P., Moore, G.W., 1971. Stratigraphic relations of Upper Cretaceous and Eocene Formations, San Diego Coastal Area, California. *AAPG Bulletin* 55, 709–722.
- Kirk, E.C., Simons, E.L., 2001. Diets of fossil primates from the Fayum depression of Egypt: a quantitative. *Journal of Human Evolution* 40, 203–229.
- Kirk, E.C., Williams, B.A., 2011. New adapiform primate of old world affinities from the Devil’s Graveyard formation of Texas. *Journal of Human Evolution* 55, 927–941.
- Lewis, P.O., 2001. A likelihood approach to estimating phylogeny from discrete morphological character data. *Systematic Biology* 50, 913–925.
- Lillegraven, J.A., 1980. Primates from Later Eocene rocks of Southern California. *American Society of Mammalogists* 61, 181–204.
- Maddison, W.P., Maddison, D.R., 2017. Mesquite: a modular system for evolutionary analysis, Version 3.2. <http://mesquiteproject.org>. <https://mesquiteproject.wikispaces.com/How+to+Cite+Mesquite>.
- Mason, M.A., 1990. New fossil primates from the Uintan (Eocene) of Southern California. *PaleoBios* 13, 1–7.
- Murphey, P.C., Dunn, R.H., 2009. *Hemiacodon engardae*, a new species of omomyid primate from the earliest Uintan Turtle Bluff Member of the Bridger Formation, southwestern Wyoming, USA. *Journal of Human Evolution* 57, 123–130.
- Murphey, P.C., Townsend, K.E.B., Friscia, A.R., Westgate, J., Evanoff, E., Gunnell, G.F., 2017. Paleontology and stratigraphy of Middle Eocene rock units in the southern Green River and Uinta Basins, Wyoming and Utah. *Geology of the Intermountain West* 4, 1–53.
- Ni, X., Li, Q., Li, L., Beard, K.C., 2016. Oligocene primates from China reveal divergence between African and Asian primate evolution. *Science* 352, 673–677.
- Rasmussen, D., Conroy, G., Friscia, A., 1999. Mammals of the middle Eocene Uinta Formation. *Vertebrate Paleontology of Utah*. Utah State Geological Survey, Salt Lake, pp. 401–420.
- Rasmussen, D.T., Shekelle, M., Walsh, S.L., Riney, B.O., 1995. The dentition of *Dyscoleleum*, and comments on the use of the anterior teeth in primate systematics. *Journal of Human Evolution* 29, 301–320.
- Robinson, P., Gunnell, G.F., Walsh, S.L., Clyde, W.C., Storer, J.E., Stucky, R.K., Froehlich, D.J., Ferrusquia-Villafranca, I., McKenna, M.C., 2004. Wasatchian through Duchesnean biochronology. In: Woodburne, M.O. (Ed.), *Late Cretaceous and Cenozoic Mammals of North America*. Columbia University Press, New York, pp. 106–155.
- Ronquist, F., Huelsenbeck, J., van der Mark, P., 2005. MrBayes 3.1 manual. Distributed with the program by the authors.
- Ronquist, F., Teslenko, M., van der Mark, P., 2012. MrBayes 3.2: efficient Bayesian phylogenetic inference and model choice across a large model space. *Systematic Biology* 61, 539–542.
- Rose, K.D., MacPhee, R.D.E., Alexander, J.P., 1999. Skull of early Eocene *Cantius abditus* (primates: Adapiformes) and its phylogenetic implications, with a reevaluation of “*Hesperolemur*” actius. *American Journal of Physical Anthropology* 109(4), 523–539. [https://doi.org/10.1002/\(SICI\)1096-8644\(199908\)109:4<523::AID-AJPA8>3.0.CO;2-U](https://doi.org/10.1002/(SICI)1096-8644(199908)109:4<523::AID-AJPA8>3.0.CO;2-U).
- Schneider, C., Rasband, W., Eliceiri, K., 2012. NIH image to ImageJ: 25 years of image analysis. *Nature methods* 9, 671.
- Simons, E.L., 1961. The dentition of *Ourayia*: Its bearing on relationships of Omomyid Prosimians, 54. Postilla Yale Peabody Museum, pp. 1–20.
- Stock, C., 1933. An Eocene Primate from California. *Proceedings of the National Academy of Sciences* 19(11), 954–959.
- Swofford, D., 2003. PAUP*: phylogenetic analysis using parsimony (* and other methods). Sinauer Associates, Sunderland, MA, Version 4.
- Szalay, F.S., 1976. Systematics of the Omomyidae (Tarsiiformes, Primates): taxonomy, phylogeny, and adaptations. *Bulletin of the American Museum of Natural History* 156, 157–450.
- Tornow, M.A., 2008. Systematic analysis of the Eocene primate family Omomyidae using gnathic and postcranial data. *Bulletin of the Peabody Museum of Natural History* 49, 43–129.
- Wagner, P., 2012. Modelling rate distributions using character compatibility: implications for morphological evolution among fossil invertebrates. *Biology Letters* 8, 143–146.
- Walsh, S.L., 1991. Eocene mammal faunas of San Diego county. *Society for Sedimentary Geology* 161–178.
- Walsh, S.L., 1996. Middle Eocene Mammal Faunas of San Diego county, California. In: Prothero, D.R., Emry, R.J. (Eds.), *The terrestrial Eocene-Oligocene transition in North America*. Cambridge University Press, New York, pp. 75–120.
- Walsh, S.L., Prothero, D.R., Lundquist, D.J., 1996. Stratigraphy and paleomagnetism of the Middle Eocene Friars Formation and Poway Group, Southwestern San Diego County, California. In: Prothero, D.R., Emry, R.J. (Eds.), *The terrestrial Eocene-Oligocene Transition in North America*. Cambridge University Press, New York, pp. 120–154.
- West, R.M., 1982. Fossil Mammals from the Lower Buck Hill Group, Eocene of Trans-Pecos Texas: Marsupialcarnivora, Primates, Taeniodonta, Condylarthra, bunodont Artiodactyla, and Dinocerata. *Texas Meml Museum Pearce-Sellers Ser Univ Texas Austin* 35.
- Westgate, J.W., 1990. Uintan Land Mammals (excluding rodents) from an Estuarine Facies of the Laredo Formation (Middle Eocene, Claiborne Group) of Webb County, Texas. *Journal of Paleontology* 64, 454–468.
- Williams, B.A., Kirk, E.C., 2008. New Uintan primates from Texas and their implications for North American patterns of species richness during the Eocene. *Journal of Human Evolution* 55, 927–941.
- Wright, A.M., Hillis, D.M., 2014. Bayesian analysis using a simple likelihood model outperforms parsimony for estimation of phylogeny from discrete morphological data. *PLoS One* 9, e109210.